University of Stavanger

Faculty of Science and Technology

Master Thesis

Study program/ Specialization: Petroleum Engineering /Drilling Technology	Spring semester, 2014 Open
Writer: Jonathan Adzokpe	…… (Writer's signatures)
Faculty supervisor: Mesfin Belayneh External supervisor : Eric Cayeux	
Title of thesis: **Hook-load Measurements made with a Draw-works as a Function of Sensor Placement and Dynamic Conditions**	
Credits (ECTS): 30	
Key words: Hook load Weight indicator Tension Friction	Pages: 88 + enclosures: 10 Stavanger, 15/06/2014

Acknowledgements

Every work of this nature does not only involve the efforts of the author, but most importantly, the mentorship and contribution from many hands behind the scenes.

First and foremost, I will want to thank God for the gift of life, and the daily supply of my needs and wants; which have sustained me to live to see this work to its completion.

I will like to also thank my parents and siblings for their love and support, though thousands of kilometers away, they have always checked up on me, prayed for me, and encouraged me through it all.

Very special to my heart are my two supervisors, Mesfin Belayneh, my university supervisor, whose consistent monitoring and push has caused me to work harder than I would have naturally wanted to. A very big thank you also goes to Eric Cayeux, my supervisor at the International Research Institute of Stavanger. Your mentorship is very much appreciated.

To whoever has contributed in any way towards the successful completion of this work, I salute you!

Stavanger, 13th June 2014

Abstract

As more oil blocks get explored for, the search and drilling for oil has become more daunting today, than ever before. Explorers and drillers have had to deal with harsh conditions of temperature, pressure, and more complex reservoir structures. Drilling wells, whether exploration or production, have also faced more challenges due to the daunting task of newer locations for oil and gas resources.

The cost of wells, the time to drill, etc. have all seen an upward spiral in recent times. One of the key parameters that greatly influences drilling efficiency, which directly impacts time and cost, is the hook load.

The hook load is measured using weight indicators which could be placed at various locations on the drilling rig. The accurate measurements of these hook load readings have been intensely researched, with the work of Luke and Juvkam being central to most of these research works.

The main pre-occupation of this thesis work was to investigate the effect of other factors on the hook load. Factors such as the weight per unit length of the drill line, dolly retraction, and mud hose and top-drive umbilicals have been modelled, and experiments carried out. These experiments have rightly confirmed that these factors have some effect on the overall hook load that is measured by the sensor at the dead line.

It has thus become obvious that the hook load that is measured is not only dependent on the weight of the drill string in the well being drilled, but other often neglected systems of the drilling rig have effect on it, somewhat.

In order to validate the model that was arrived at as a correction to the already existing model, experiments were carried out on a highly accurate basis. These experiments have confirmed what was arrived at with the model.

Table of Contents

Contents

1 Introduction

The accurate measurement and prediction of hook load and other parameters is very important for safe drilling operation. According to Luke and Juvkam [20], the instrument used by industry personnel to measure the hook load at any given point in time during drilling is the weight indicator. Therefore, the suspended weight in the hook is dependent on the dead line tension. [27]

The weight indicator is designed to operate on a hydraulic load cell which could be attached to the dead line or even made it to be a part of the dead-line anchor. [19]

The position of the measurement determines the accuracy of the hook load. When measurement is performed at the fast line, there are several factors which the model needs to account for.

This thesis seeks to investigate other factors that could likely affect the hook-load measurements made with a draw-works as a function of dynamic conditions. This becomes even more crucial as hook load is one of the important drilling parameters in a typical drilling operation on the rig.

1.1 Background

Drilling in the oil and gas industry is carried out with the drilling rig. The drilling rig consists of various systems that operate to facilitate the drilling process. These systems include the following;

1. Hoisting systems
2. Power system
3. Circulating system
4. Rotary system
5. Well control &monitoring system

In this report, the main focus will be on the hoisting system, which is one of the most integral systems that make up the drilling rig. The hoisting system consists of the draw works, whose main function is to provide a means of lifting and lowering the traveling blocks; the derrick, which serves as the structure to provide support for the equipment used to lift and lower the drill string out and into the wellbore; it also consists of the crown and travelling blocks.

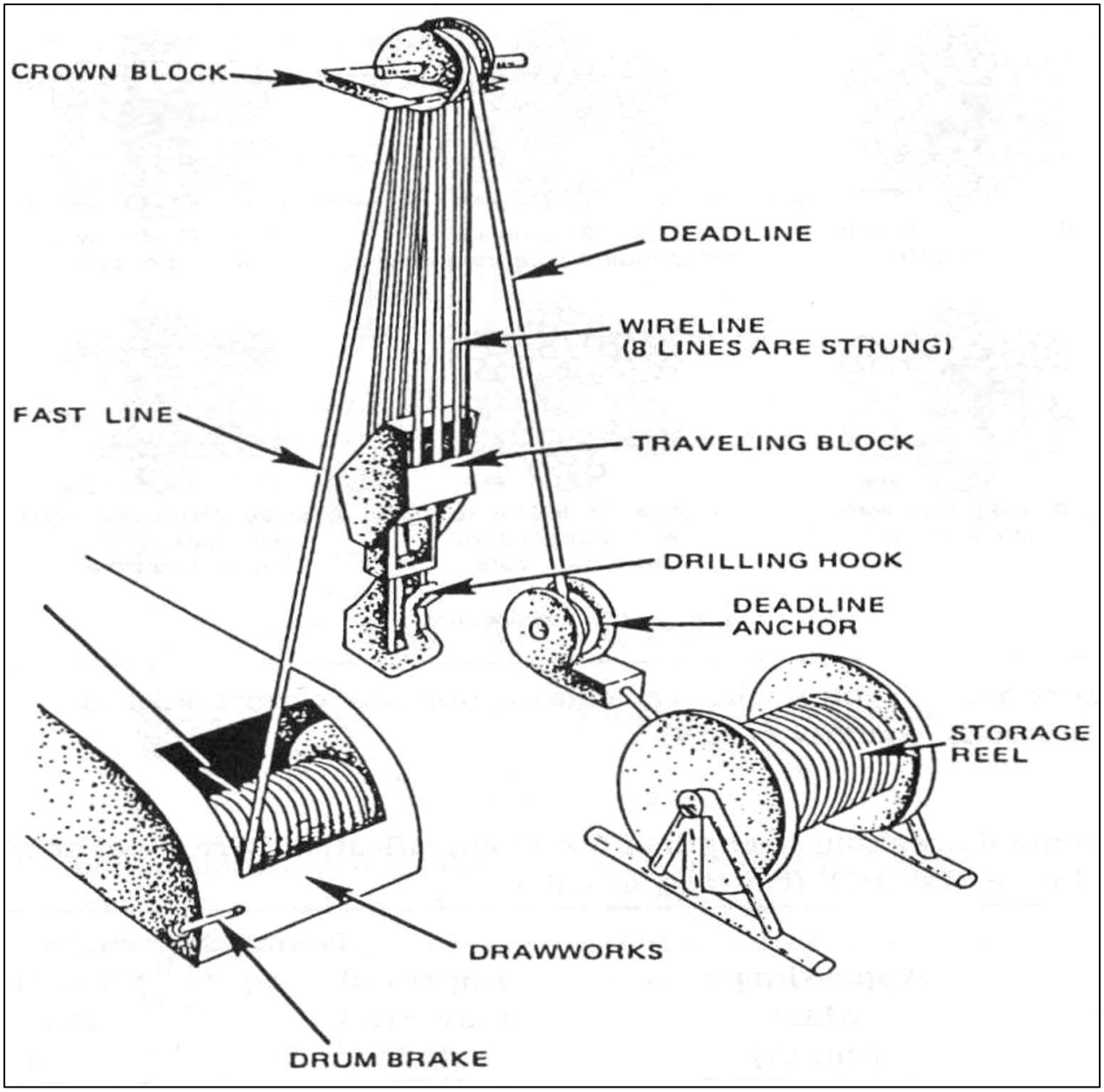

Figure 1: The diagram of a hoisting system [17]

Following discrepancies in theoretical and experimental studies, it was demonstrated that hook load depends on sheave friction, direction of block movement, and previous movement history. However, the hook load readings that are observed are normally up to 19% higher than what is predicted by the method used by the industry at the time.

This led to the work of Luke and Juvkam, who set out to determine true hook load and line tension under dynamic conditions which they presented in the paper. [19]

In the results of their research which they had tested on field data, they found the following;

a. The rig they used in validating their experimental results had a top drive of weight approximately, 80,000 lbf. After zeroing out the weight indicator, the blocks were raised to know what the weight indicator would read. From their observation, the weight indicator read 71,000 lbf, which is 12.7% lower than the true weight of the top drive. This error simply proved that the weight indicator displayed the wrong weight readings.
b. Also, as the blocks were lifted and lowered, weight indicator readings of 52,600 lbf and 58,600 lbf respectively were recorded.

From their research, Luke and Juvkam had proven that the method of predicting hook and derrick loads at the time was inaccurate due to its wrong assumptions which led to a higher degree of discrepancies.

From their study they also came to a conclusion that tension at the dead-line is dependent on the block movement. However, it is dependent on the previous block-movement history under static conditions. Another observation is that an actual hook load is independent on the direction of the traveling-block-movement under steady-state conditions. Also, hook load prediction with tension in the dead-line is dependent on the direction of traveling-block-movement.

The experimental observations also reveal that a gradual reduction in tension when coming out of the hole from the fast to dead line. On the contrary in lowering the traveling block, the dead line experiences a higher tension reading as compared to the fast line.

1.2 Problem formulation

In addition to experimental study, Luke and Juvkam's work (1993) presented a hook load model, which took no account of the possible effect of weight of drill line, the position of block and the speed of block and the rotational velocity of the rotating pulleys. The authors considered the sheave friction in terms of sheave friction efficiency.

Mme et al (2012) have experimentally observed that block acceleration have effect on the hook load. According to their observation an increase in acceleration increases the hook load and the

decrease in acceleration decreases hook load. As can be seen on figure 2, for zero acceleration the hook load is constant.

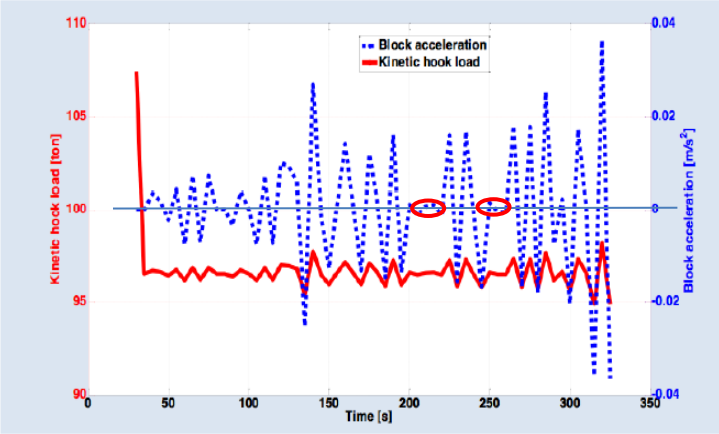

Figure 2 - An observed correlation between hook load and block acceleration [23]

As can be seen from figure 2, the red oval shapes indicate points of zero acceleration which indicates constant velocity. At such points of zero acceleration (constant velocity), hook load readings are fairly constant.

This thesis will therefore address questions like;

- What is the effect of the weight of drill lines?
- Has the retraction force during dolly retraction any effect on the total hook load readings?
- Does the tension exerted by the mud hose and top-drive umbilical have any impact on the overall resulting hook load?

1.3 Scope and objectives

With a hoisting system based on a draw-works, the top of string force (i.e. the hook load) is, in most cases, indirectly measured by placing a sensor either at the level of the deadline, or the crown-blocks, or inside the top-drive or possibly in the draw-works itself. Experience shows that the derived hook load is not only reflecting the top of string force as desired but also the effect of the additional forces generated by the hoisting system.

The sources of the deviations are the following:

a. Length of drill-line spooled out as a function of the traveling equipment position.
b. Friction between the drill-line and the sheaves of the crown blocks and traveling blocks as a function of load and velocity.
c. Tension exerted on the drill-line when the dolly is retracted as a function of the dolly position.
d. Friction between the dolly and its rails as a function of eccentricity (dolly retracted or extended), elevation of the dolly, load, and velocity.
e. Tension exerted by the mud hose and umbilical connected to the top-drive as a function of the traveling equipment position, the mud density and whether the mud hos is filled or empty (relation to last fluid circulation and opening and closing of iBOP).

2 Drilling equipment and drilling parameters

This chapter presents drilling equipment, with more emphasis on the hoisting system. It also touches on the various drilling parameters that affect drilling efficiency.

2.1 Types of drilling equipment

Drilling rigs are presently either draw-works or ram-rig operated.

2.1.1 The draw-works-operated rig

A draw-works is primarily the machinery purposed for hoisting in this type of drilling rig. Its main function is to facilitate a means of lifting and lowering the traveling blocks which hold the drill string. A drilling line is wound on the drum of the draw-works. This drill line then extends to the crown block located at the top of the derrick, and traveling blocks. This allows for the up and down movement of the drill string whiles the drum turns [14].

The drill line which extends from the draw-works atop the crown block is called the “fast line.” The drill line from the crown block then enters the sheaves of the crown block and makes a number of passes between the crown and traveling blocks pulleys. This creates a mechanical advantage which helps to lift very heavy loads with relatively smaller force. The line exits the last sheave on the crown block and is fastened to the leg of a derrick on the other side of the rig floor. This section of the drilling line is called the “dead line” [13].

A modern-day draw-works has five main component parts. These include the motor(s), the drums, the brake, the reduction gear, and the auxiliary brake. The motors are designed to be either alternating current (AC) or direct-current (DC)-motors, or the draw-works could also be connected to diesel engines directly using chain-like belts which are metallic.

The number of gears depends on the needed speed. There could be one, two, or three speed combinations. The main brake, which is usually operated manually by a long handle, could be a disc brake, a friction band brake or a modified clutch. It serves as a parking brake when no further motion is required. The auxiliary brake is connected to the drum, and which helps to absorb the energy that is released when heavy loads are being lowered. The auxiliary brake may

employ the use of water-turbine-like apparatus or eddy current rotors to convert the kinetic energy released due to a downward-moving load being stopped to heat energy.

Winches are located on each side that provides a means of activating the tongs which are used to couple and uncouple threaded pipe members [13].

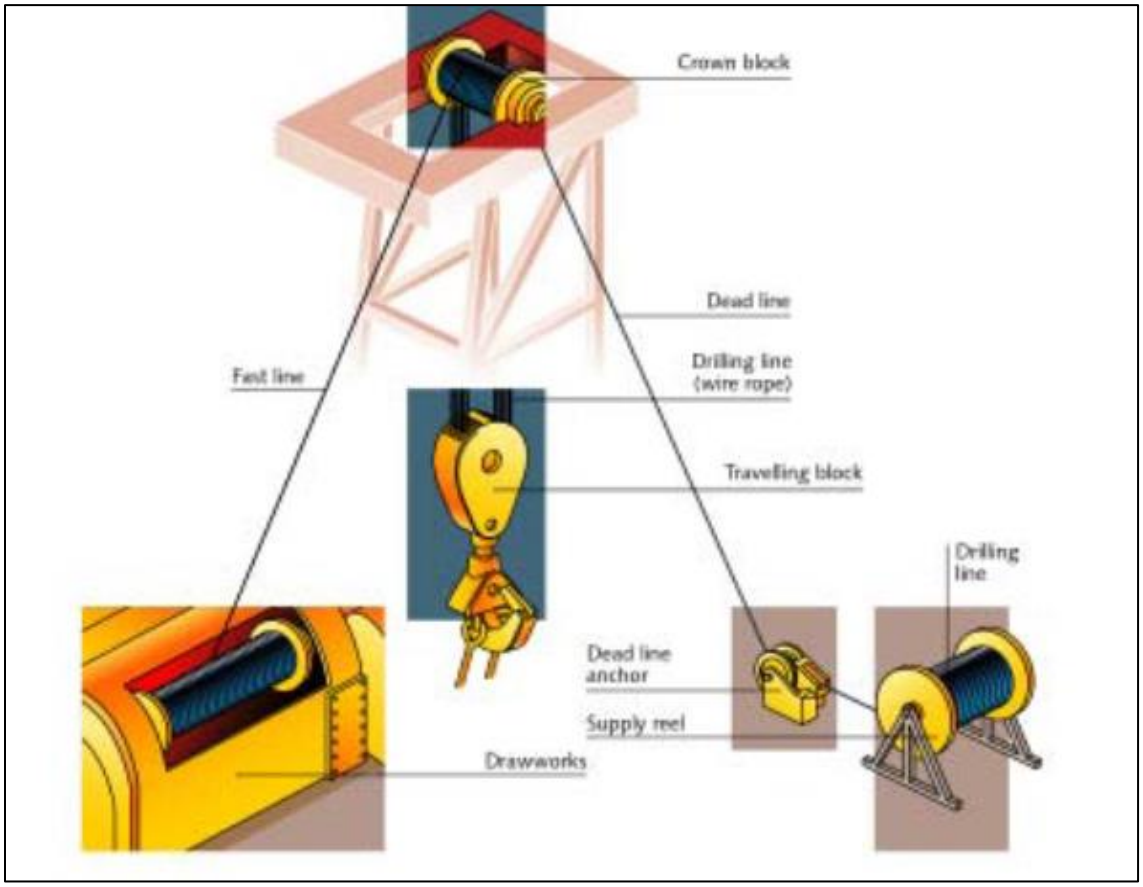

Figure 3 - The draw-works-operated rig [13]

2.1.2 Ram rig

A second type of hoisting system is the ram rig. Hoisting and lowering operations with the ram rig is carried out using two hydraulic cylinders which are also called rams. These rams are used instead of the conventional draw-works and derrick. With a ram rig, the hoisting lines are of a fixed length, parallel, and wires with one end and anchored at the drill floor, and the other end at the top drive.

The hoisting lines are designed to run over the sheaves of the yoke, thus transforming the push originating from the rams to an upward lifting force to the top drive and the guide dolly. The distance of travel and the top drive speed are twice that of the rams. The maximum stroking velocity of the rams is 1 m/s, hence making the top drive to travel at a velocity of 2 m/s.

The powering of the ram rig is achieved by the means of a central Hydraulic Power Unit (HPU). This unit has eight to fourteen pumps which are of similar/equal capacity. Any of the eight to fourteen pumps can help achieve a full hoisting force, but with a lower speed.

This means that power can be used efficiently, and also be saved for the majority of drilling operations. The pumps are of variable displacement types and are powered by alternating current motors with constant speed. An additional flow could be supplied by an accumulator, which acts as a reservoir during the performance of a passive heave compensation.

2.1.2.1 The operation of the ram rig

The hoisting of loads could be done by allocating the required number of pumps for hoisting through the operator stick, thus giving the set-point for the pump controller. This way, the pumps will give an output flow proportional to the stick input. The pump flow is proportional to the cylinder speed and that of the dolly. The load desired to be lifted primarily determines the pressure.

All loads are hoisted with equal speed and accuracy within the limitations of the pressure of the pumps. The valve blocks in the near vicinity of the cylinder serve two purposes; first, it is meant to secure the load when in a parked position and, secondly, to shift the cylinder in order to act in the regeneration mode. This mode of regeneration shifts the cylinder, thus acting as a plunger cylinder. With the cylinder geometry, this indicates a double of the speed and half of the load with the same available power.

2.1.2.2 Handling of pipes with a ram rig

Handling of pipes with a ram rig is achieved with a pipe handling mast. In order to offer a safe and hands-free drilling operation, pipe handling system which is fully automated is used. On location, the pipe handler mast is lifted to a vertical position using raising bars and skid jacks, and then ready for operation.

The head of the gripper employs a wedge design with safety latches to enable vertical and horizontal handling. In this type of pipe-handling mechanism, tubulars of different sizes are picked up without having to change claws. Also, the gripper head engages on the tubulars flush area and is independent on tool joints. The tubulars are picked up using the pipe handling machine.

This is done by extending the arm to the center position of the well, then gripping the pipe, lifting off the stick up, turning to fingerboards on either side of the pipe handling mast, and then lowering down to simple “setback mast”. All of the tubulars weight in the setback is therefore supported on the ground.

Figure 4 - The pipe handling machine [24]

2.1.3 The anatomy of the hoisting system

The hoisting system of drilling rigs is made of a simple block-and-tackle system of pulleys with drill line strung around the pulleys.

The block-and-tackle arrangement of the hoisting system provides the needed mechanical advantage capable of handling heavy loads in an easier fashion. In other words, the mechanical advantage is the ratio of the load that is supported by the traveling block to the tension in the fast line. [19]

2.2 Drilling Parameters

For a better drilling experience devoid of many drilling challenges, certain parameters are very important, and their optimization could likely lead to minimal drilling-related problems. Some of these drilling parameters include;

a. Weight On Bit (WOB)
b. Revolution Per Minute (RPM)
c. Mud flow rate
d. Rate Of Perforation (ROP)

2.2.1 Weight On Bit (WOB)

Weight On Bit (WOB) is the amount of downward force that is exerted on the drill bit during drilling. WOB is provided by the drill collars, which are thick-walled pipes that are manufactured from steel. These steels are normally plain carbon steel. They could also be made of non-magnetic premium alloys or non-magnetic nickel-copper alloy.

Due to their large weight, usually in thousands of pounds, gravity acts on the collars to provide the needed downward force in order for the bits to efficiently break formation rocks. For a driller to be able to accurately control the amount of downward force applied to the bit by the drill collars, he/she monitors the weight on the surface that is measured when the drill bit is just off the wellbore bottom. [3]

2.2.2 Revolution Per Minute (RPM)

The RPM is the amount of times the drill bit rotates in one minute. There are two principal elements that must be taken into consideration when determining the optimum RPM.

a. The diameter of the bit being used.
b. The type of rock being drilled through.

Using an RPM that is slower than expected will lead to unnecessary wear and pressure on the drilling bit. This slower-than-expected RPM means that the drilling pressure will be too high; hence the drill bit might break.

An RPM that is too fast will also result into chatter and vibration on both the drilling bit and formation being drilled. Such a phenomenon could lead to a high heat being generated and could likely damage the cutting edges of the drilling bit. [6] As such, an optimum RPM will be ideal for efficient drilling.

2.2.3 Mud flow rate

The drilling mud is one of the most critical elements during drilling operation. The mud is pumped from the mud pits, using pumps and through the drill string down through the nozzles of the drill bit where it is expected to cool and clean the drill bit. [4]

Also, one of the key importance of the drill mud is to transport drill cuttings to the surface through the annulus; that is, the space between the drill string and the wellbore.

The drill mud exhibits various properties such as;

a. Flow rate
b. Density
c. Viscosity
d. Yield point
e. Gel strength, etc.

To remove cuttings efficiently, the circulating rates (mud flow rate) should be sufficient enough in order to overcome the force of gravity that is acting on the cuttings. [5]

2.2.4 Rate of Penetration (ROP)

The rate of penetration (ROP) is defined as the speed at which the drill bit breaks the formation rock to increase the depth of the borehole. It could also be known as penetration rate or drill rate. ROP is usually measured in feet per minute (ft/min) or meters per hour (mph). In some instances, it could also be expressed in minutes per foot (min/ft).

In general sense, the rate of penetration (ROP) increases in fast formations such as sandstone. It, however, decreases in slow formations like shale. The decrease in slow shale formations is due to overburden stresses and diagenesis.

Management of ROP: The importance of ROP has made it essential for proper management to yield efficient drilling operations; thus reducing non-productive time (NPT), and hence the cost of drilling.

2.3 Problems encountered during drilling

The drilling process is one that is not devoid of problems. Some of the common problems encountered by drillers regularly include the following;

2.3.1 Drill-string buckling

Drill string buckling is one of the potential problems that drillers are bound to face during the drilling process. Buckling in the drill-string occurs if compressive stresses acting on the string are greater than the internal strength of each pipe component making up the string. This thus causes pipe failure.

2.3.2 Stuck pipe

A stuck pipe situation occurs when roc cuttings present in the wellbore during drilling are not transported efficiently from the well annulus to surface. This is due to the lack of enough cutting velocity in the wellbore. It can also occur when mud properties in the wellbore is poor. When pumps are switched off, cuttings fall down to the bottom of the wellbore as a result of gravitational force. This, invariably, leads to a stuck pipe situation. [2]

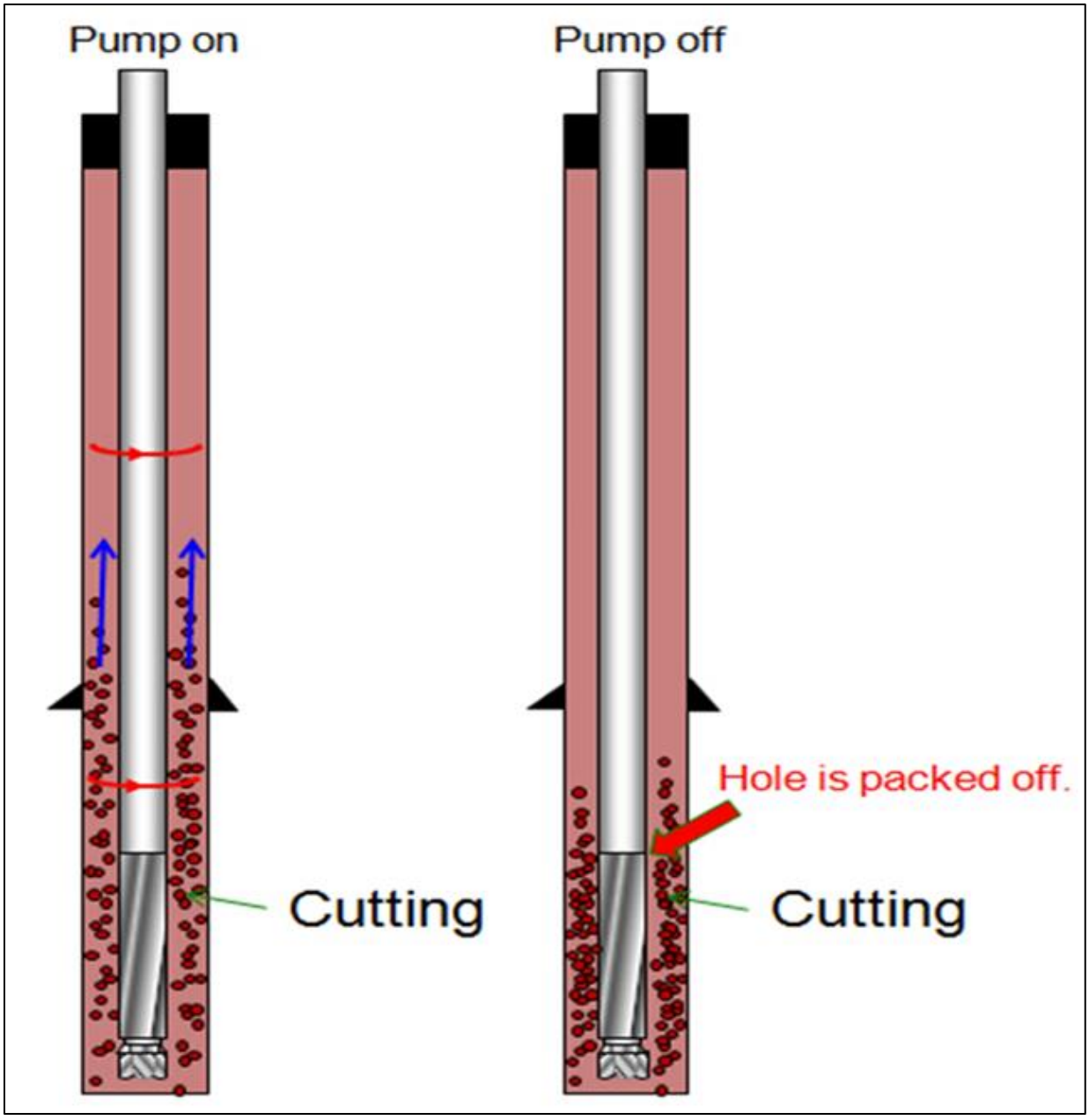

Figure 5 - A packed-off leading to stuck pipe when pumps are switched off [1]

3 Theory

3.1Torque and Drag Theory

The torque and drag theory is the basis for the analysis of drilling such as tripping in/out and installation of liner and casing. The hook load is determined from the drag and weight of the drill string. Therefore, this section reviews the type of drag and the next section will look at the hook load determination.

3.1.1 Drag model

The drill string mechanics module computes loads in drill string in tripping, and drilling condition. In addition to computing the buckling and tensile load limits. The main objective is to describe the allowable loads on drill string, which is bounded by the buckling and the tensile limits. The physics behind the torque and drag model is obtained by force balance. When calculating buckling loads and torque and drag forces, all loads must be computed with respect to a given well geometry (inclination, azimuth and measured depth). The drill string is assumed to be divided up into a number of short jointed segments (cells) through which the transmission of tension, compression, and torsion are allowed.

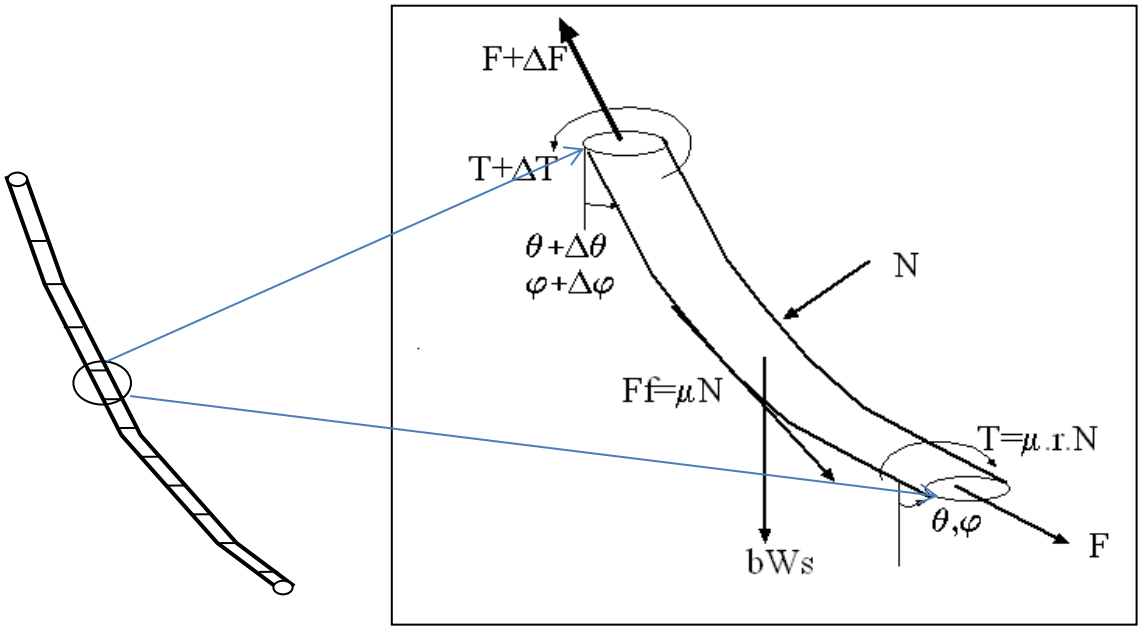

Figure 6 - A simple free-body diagram of a drill string segment with respective loads

Applying the condition of equilibrium along the axial and normal directions, the effective force along the axial direction is, according to [21]:

$$\frac{dF}{ds} = \pm\mu_a N + \beta w_s cos\theta \tag{3.1}$$

Johancsik et. al. (1984) derived the normal force in any curved well geometry that shows variation in inclination and azimuth [1]:

$$N_i = \sqrt{\left(\beta w_{si} sin\left(\frac{\theta_{i+1}+\theta_i}{2}\right) - F_i\left(\frac{\theta_{i+1}-\theta_i}{S_{i+1}+S_i}\right)\right)^2 + \left(F_i sin\left(\frac{\theta_{i+1}+\theta_i}{2}\right) - F_i\left(\frac{\varphi_{i+1}-\varphi_i}{S_{i+1}+S_i}\right)\right)^2} \tag{3.2}$$

When drilling at various angular rotational speeds and when tripping in/out, the drill string is at various axial speeds. These dynamic parameters affect the axial and tangential friction coefficients, and will be considered in the torque and drag model as the following [21]:

The axial friction factor: $\mu_a = \mu \sin a$

Where the angle α is given by $\tan\alpha = \frac{v_a}{r\Omega}$. r is the drill string radius, Ω is the angular velocity of rotation and v_a is the axial speed. v_a is defined positive for tripping in and drilling, and negative for pulling out:

$$F_{i+1} = F_i + \sum_{i=1}^{n}\left[\beta w_i \cos\left(\frac{\theta_{i+1}+\theta_i}{2}\right) \pm \mu_i N_i\right](S_{i+1} - S_i) \tag{3.3}$$

$F_{a(i)}$ is the bottom weight when integrating from bottom to top. The positive sign is for run out of the hole and the negative sign is run into the hole.

3.1.2 Torque model

The torque loss per unit length for both buckled and non-buckled string is given as:

$$T_{i+1} = T_i + \sum_{i=1}^{n} \mu_t r_i . N_i . (S_{i+1} - S_i) \tag{3.4}$$

$$\mu_t = \mu \cos \alpha$$

where the tangential friction factor is always positive. N_i is the contact force per unit length.

3.2 Hydrodynamics force effect on Hook load

Effect of Hydrodynamic Viscous Force

Drilling fluid circulation has loading effect on the drill string. The hydrodynamics forces are due to flow and viscous part. The fluid flow has effect on the torque and drag loading. [11] The force can be included on the first order differential equation and modifying equation 3.1 as:

$$\frac{dF}{ds} = \pm \mu_a N + \beta w_s \cos \bar{\theta} + \frac{dF_{fl}}{ds} \tag{3.5}$$

In [25], Maidla and Wojtanowicz (1987) derived viscous force effect on drag force. The hydrodynamic viscous drag force coupled with the drag equation [15]:

$$F_{fl} = \frac{\pi}{4} \sum_{i=1}^{n} \left(\frac{\Delta P}{ds} \right) \Delta s_i d_i^2 \tag{3.6}$$

Where the pressure loss term with fluid velocity and density in the annulus is given as:

$$\frac{\Delta P}{ds} = \frac{f \rho V_{av}^2}{D - d} \tag{3.7}$$

Where *D* is the well diameter and *d* is the outer diameter of the drillstring.

The coefficient f in laminar flow is given by the Reynolds number N_{Re} as:

$$f = \frac{16}{N_{Re}} \tag{3.8}$$

To find the turbulent friction the equation below is used:

$$\frac{1}{\sqrt{f}} = -4\log_{10}\left[\frac{0.27\varepsilon}{D_{eff}} + 1.26^{N^{-1.2}}/\left(N_{Re,G}f^{1-N/2}\right)^{N^{-0.75}}\right] \tag{3.9}$$

Where:
ε is wall roughness.
Reynolds number:

$$N_{Re} = \frac{\rho v D_{eff}}{\mu_{app}} \tag{3.10}$$

In eq. 3.10, D_{eff} is the effective diameter. μ_{app} is the apparent viscosity.

3.3 Field hook load data vs various effects

Aadnoy et al. (2010) derived 3D analytical model and the model with field tripping out hook load data obtained from North Sea. The authors have compared their 3D model along with other three models against real time hook load data. The results of the comparisons using 0.2 friction factor on the entire drilling formation is shown in Figure 7.

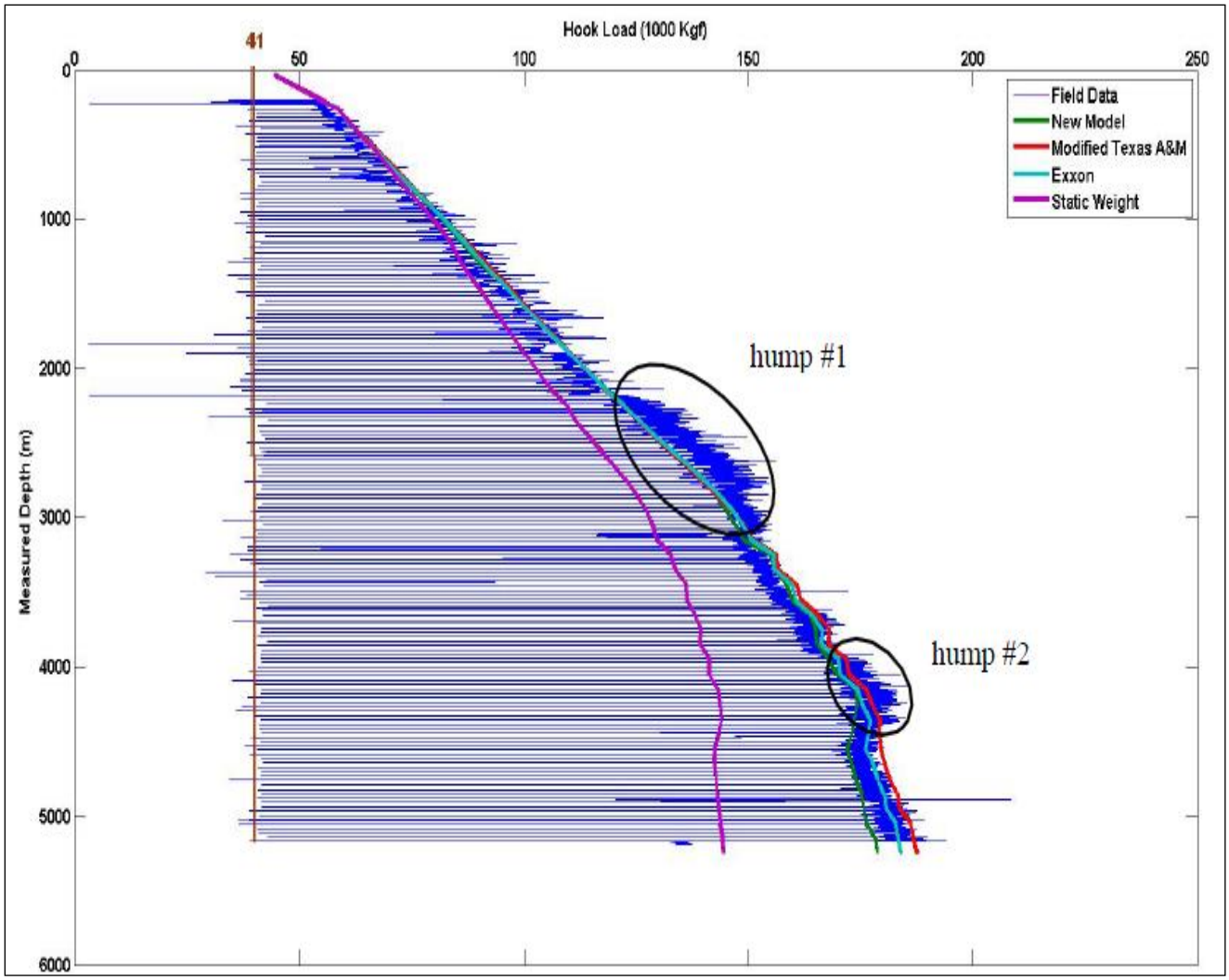

Figure 7 - Comparison of models and field hook load data for tripping out [21]

The models shows quite good match with the real time field data except two sections. These two humps section are where the well builds up angle. The Johancsik model gives a good match for the last length of the well, below hump #2, while the new 3D model is below the real time hook loads.

During running operation, the drill string in reduction and filling process is performed throughout the operation. This is due to the mud level reduction. The second case example shows the tripping in hook load data. As shown on the figure, a periodically occurring stepwise event that represents the drill string has been filled nearly every 1000m MD in the string run. On the

graph, one can observe a step increase transition, which is an indication that the drill string is filled drilling fluid.

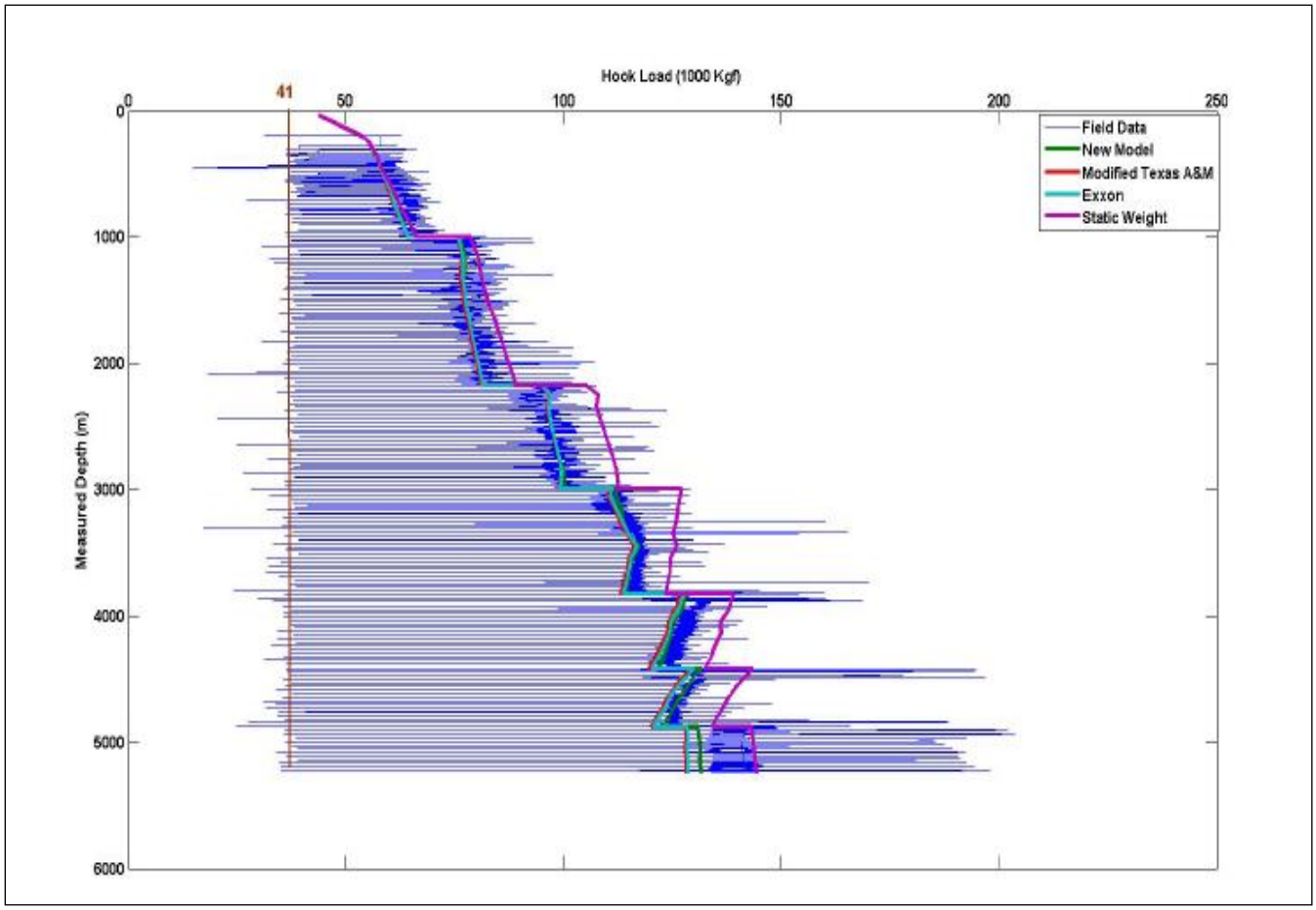

Figure 8 - Comparison of models and field hook load data for tripping in [21]

As can be seen, the model captures the most part of the drilling depth up to 3000 m MD. Afterwards in a deeper measured depth the predictions deviates from the measured data. The authors used a friction factor of 0.1, which the deviation reduced. The friction factor is among others parameters which affect the hook load. [8]

The models are derived based on several simplified assumption and soft string model. [8]

3.4 Hook load

3.4.1 The theory behind the hook load (HKL)

There are several approaches to define the suspended weight in the hook. According to [23], the hook load is the "sum of vertical components of the forces acting on the drill string attached to the hook."

3.4.2 Sensor measurement of HKL

The hook load is normally determined using sensors which are located at various positions on the drilling rig. These sensors were adapted relatively earlier in the life of the oil and gas industry in order to implement drilling operations. According to [27], John Sharpe was issued with the first weight indicator patent in 1906.

Over the decades, there has been an increased use of electronic sensors till date. However, the Martin-Decker diaphragm-type weight indicator, which was developed in 1926, has been in extensive use. [28]

Today's hoisting systems on different drilling rigs implement the use of electronic sensors, which are often located in the draw works and in the travelling block. [27]

3.4.3 Importance of HKL

According to [19], monitoring the HKL is a very essential component in the drilling process. This is because the information obtained from monitoring the HKL helps to alleviate the occurrence of such drilling-related issues as drill line breaking, and "pulling the rig in."

Each of the above mentioned conditions is likely caused by an over-pull that is exerted on by the draw works on the fast line. This is as a result of not knowing the true tension in the cable that is present in the block-and-tackle arrangement that is used to support the drill string.

3.5 Earlier works on the hook load

There have been earlier works on hook load that were spearheaded by Dangerfield in 1987 and Luke and Juvkam in 1993. Dangerfield essentially made a mathematical analysis of the resistance due to friction that is present on the hoisting system.

3.5.1 Dangerfield's work on active and inactive dead-line sheaves

In his work, he posited that there are two types of dead-line sheaves that existed; namely, the inactive and active sheaves. He went on to stress that for an active sheave on the dead-line, there is free rotation on the sheave that the dead line passes over in the crown block and back to the traveling block.

Dangerfield further stated that this condition will result in a tension differential in the lines present on either side of the sheave due to frictional resistance. In the case of an inactive dead-line sheave, no friction will be experienced by the sheave located in the crown block over which the dead line passes. [19]

This therefore means that, the dead and "first" line tensions between blocks is the same.

Since the sum of the tensions in all lines present in the system and the derrick load are equal, then the hook load can be said to be the sum of the tensions present in the lines between each block. With this background, Dangerfield was able to generate geometric series from his analysis. [19]

3.5.2 Luke and Juvkam's work

The hook load prediction, according to the accepted practice in the oil and gas industry, is an assumption based on the understanding that the tensional force present in the lines between the blocks and in the dead line are the same; irrespective of the direction of movement of the block.

Along similar line of thought, it is also assumed that the fast line tension and those in other lines are the same. Luke and Juvkam therefore set out to investigate the validity of the above stated assumptions in their paper.

To be able to evaluate the different hook-load, line-tension, and derrick-load prediction models, an experimental working rig was set up and equipped with travelling block, crown block, draw works, a data acquisition system and load monitoring devices.

3.5.2.1 Inactive Dead-Line Sheave

An inactive dead-line sheave is the sheave located in the crown block which is frictionless and over which the dead/line passes. This thus results in the dead-line and first line between blocks to be the same. [19]

When raising the blocks,

$$F_d = F_{dl}[1 + (1/e^n) - 2e]/(1 - e)$$

$$W = F_{dl}e[1 - (1/e^n)]/(e - 1) \quad (3.11)$$

$$F_{fl} = F_{dl}/e^n$$

$$F_{fl} = W(1 - e)/e(1 - e^n)$$

When lowering the blocks,

$$F_d = F_{dl}(2 - e - e^{n+1})/(1 - e)$$

$$W = F_{dl}(1 - e^n)/(1 - e) \quad (3.12)$$

$$F_{fl} = F_{dl}e^n$$

$$F_{fl} = We^n(1 - e)/(1 - e^n)$$

3.5.2.2 Active Dead-Line Sheave

In the case of an active dead-line sheave, it refers to the "sheave over which the dead-line passes in the crown block on its way back to the traveling block is free to rotate. This condition causes a differential between the tensions in the lines on either side of the sheave because of frictional resistance". [19]

When raising the blocks

$$F_d = F_{dl}(1 - e^{n+2})/(1 - e)e^{n+1}$$

$$W = F_{dl}(1 - e^n)/(1 - e)e^n \quad (3.13)$$

$$F_{fl} = F_{dl}e^n$$

$$F_{fl} = W(1 - e)/e(1 - e^n)$$

When lowering the blocks,

$$F_d = F_{dl}(1 - e^{n+2})/(1 - e)$$

$$W = F_{dl}e(1 - e^{n})/(1 - e) \quad (3.14)$$

$$F_{fl} = F_{dl}e^{n+1}$$

$$F_{fl} = We^{n}(1 - e)/(1 - e^{n})$$

Where

- $e =$ individual sheave efficiency
- $F_d =$ derrick load, mL/t^2, lbf
- $F_{dl} =$ dead-line tension, mL/t^2, lbf
- $F_{fl} =$ fast-line tension, mL/t^2, lbf
- $n =$ number of lines between blocks
- $W = hook\ load, mL/t^2$, lbf

4 Modelling

The model presented in this chapter is fully referenced to the work in [22].

This thesis report will attempt to investigate what effect factors such as the weight of the drill line, dolly retraction and mud and top-drive umbilicals have on the overall hook load reading. Experience shows that the derived hook load is not only reflecting the top of string force as desired but also the effect of the additional forces generated by the hoisting system. The sources of the deviations are the following:

a. length of drill-line spooled out as a function of the traveling equipment position,
b. friction between the drill-line and the sheaves of the crown blocks and traveling blocks as a function of load and velocity,
c. tension exerted on the drill-line when the dolly is retracted as a function of the dolly position
d. friction between the dolly and its rails as a function of eccentricity (dolly retracted or extended), elevation of the dolly, load and velocity
e. tension exerted by the mud hose and umbilical connected to the top-drive as a function of the traveling equipment position, the mud density and whether the mud hos is filled or empty (relation to last fluid circulation and opening and closing of iBOP)

As a start, the author derives the Luke and Juvkam-Wold equations found in their paper, "Determination of True Hook Load and Line Tension Under Dynamic Conditions." Details can be found in the appendix. Luke and Juvkam-Wold arrived at the following equations under each sub-section;

4.1 Model Improvement Approach

To be able to investigate the effect of the listed factors on the hook load, here are the steps to be followed;

1. The effect of the linear weight of the drill-line is added. It will then be found how this affects the measurement at the dead-line, crown block, and draw-works as a function of the number of pulleys, and block position.

2. The effect of the tension of the mud hose on the top-drive will also be added: how this affects the measurement at the dead-line, crown block and draw-works as a function of the block position is found, and compare with the effect of the number of pulleys.
3. The effect of the centrifugal force on the drill-line around the pulleys is added: checks will be run on how this affects the measurements as a function traveling equipment velocity.
4. The effect of dolly being retracted or extended will then be added as well: how this affects the measurements as a function of the block velocity and position will be checked.4.3 Model Improvement Derivation

4.2 Effect of the linear weight of drill line

In this derivation, it will be assumed that there are no effects due to acceleration.

Let's denote the distance between the sensor on the dead-line and the closest block B1 by L. Thus, the tension, T_1, at the level of the block is;

$$T_1 = -(F_{dl} + Lg\partial_s m_{dl})$$

Where,

F_{dl} is the dead-line tension

g is the acceleration due to gravity

$\partial_s m_{dl}$ is the drill-line linear weight (s refers to the curvilinear abscissa)

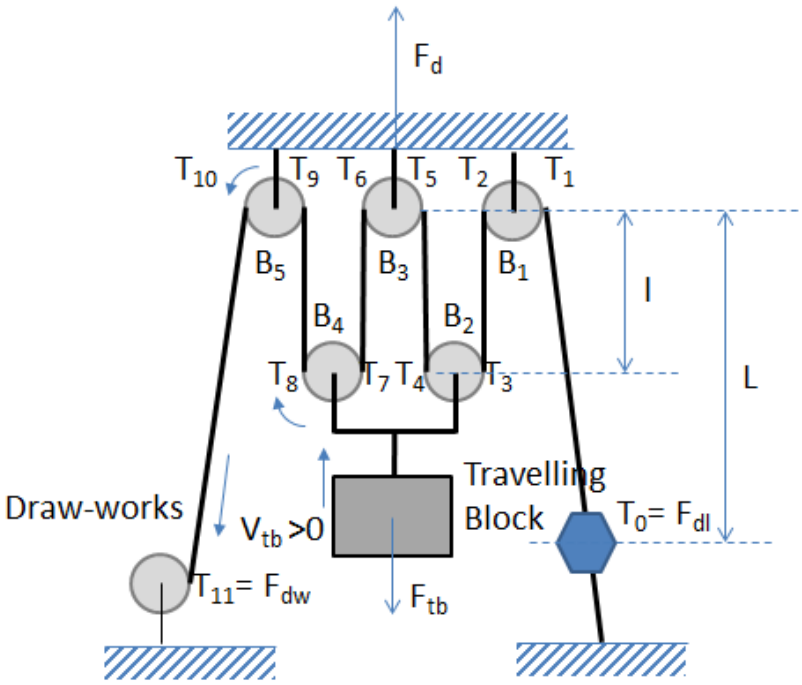

Figure 9 - Block-and-tackle schematic showing the various tensions present along the drilling line [22]

It should be noted however that block B_1does not rotate, thus there is no loss of tension which makes both tensions on each side of the block, equal. Hence, $T_2 = T_1$. On the right side of block B_2 however, the tension T_3 becomes;

$$T_3 = F_{dl}(L - l)g\partial_s m_{dl} \qquad 4.1$$

Where,

l is the distance between the traveling and crown blocks

The tension on the opposite side of B_2, T_4 is dependent on the direction of the traveling-equipment-movement.

Thus,

$$\begin{cases} \forall v_{tb} > 0, T_4 = \varepsilon^{-1}T_3 = \varepsilon^{-1}(F_{dl} + (L - l)g\partial_s m_{dl}) \\ \forall v_{tb} < 0, T_4 = \varepsilon T_3 = \varepsilon(F_{dl} + (L - l)g\partial_s m_{dl}) \end{cases} \qquad 4.2$$

Where,

$v_{tb}$is the traveling block velocity, which is defined positive for upward movement.

Following the aforementioned, we can go ahead to derive all other tensions for upward movement, thus, $\forall v_{tb} > 0$

$$\forall i \in \left[1, \frac{n}{2} - 1\right], T_{4i-1} = \left(\varepsilon^{-21+2} F_{dl} + g\partial_s m_{dl} \left(L - l \sum_{k=0}^{2i-2} (-1^k)\varepsilon^k \right) \right)$$

$$\forall i \in \left[1, \tfrac{n}{2} - 1\right], T_{4i} = \varepsilon^{-2i+1} \left(F_{dl} + g\partial_s m_{dl} \left(L - l \textstyle\sum_{k=0}^{2i-2} (-1)^k \varepsilon^k \right) \right) \qquad 4.3$$

$$\forall i \in \left[1, \frac{n}{2} - 1\right], T_{4i+1} = -\varepsilon^{-2i+1} \left(F_{dl} + g\partial_s m_{dl} \left(L - l \sum_{k=0}^{2i-1} (-1)^k \varepsilon^k \right) \right)$$

$$\forall i \in \left[1, \frac{n}{2} - 1\right], T_{4i+2} = -\varepsilon^{-2i} \left(F_{dl} + g\partial_s m_{dl} \left(L - l \sum_{k=0}^{2i-1} (-1)^k \varepsilon^k \right) \right)$$

Where n denotes the number of lines including the fast and dead-lines

Also, the tensions for downward movements ($\forall v_{tb} < 0$);

$$\forall i \in \left[1, \frac{n}{2} - 1\right], T_{4i-1} = \left(\varepsilon^{2i-2} F_{dl} + g\partial_s m_{dl} \left(L - l \sum_{k=0}^{2i-2} (-1^k)\varepsilon^k \right) \right)$$

$$\forall i \in \left[1, \tfrac{n}{2} - 1\right], T_{4i} = \varepsilon^{2i-1} \left(F_{dl} + g\partial_s m_{dl} \left(L - l \textstyle\sum_{k=0}^{2i-2} (-1)^k \varepsilon^k \right) \right) \qquad 4.4$$

$$\forall i \in \left[1, \frac{n}{2} - 1\right], T_{4i} = \varepsilon^{2i-1} \left(F_{dl} + g\partial_s m_{dl} \left(L - l \sum_{k=0}^{2i-2} (-1)^k \varepsilon^k \right) \right)$$

$$\forall i \in \left[1, \frac{n}{2} - 1\right], T_{4i+2} = -\varepsilon^{2i} \left(F_{dl} + g\partial_s m_{dl} \left(L - l \sum_{k=0}^{2i-1} (-1)^k \varepsilon^k \right) \right)$$

We will then need to calculate the force on the traveling block (F_{tb}) by writing the balance of forces on the traveling equipment;

$$F_{tb} = -\sum_{i=1}^{n/2-1} (T_{4i-1} + T_{4i})$$

For the derrick load, F_d, we have,

$$F_d = -\sum_{i=1}^{n/2-1}(T_{4i+1} + T_{4i+2}) \qquad 4.5$$

The tension on the fast line (F_{fl}) at the level of the draw-works is;

$$F_{fl} = T_{2(n-1)} - Lg\partial_s m \qquad 4.6$$

4.3 Effect of the tension of the mud hose and umbilicals on the top-drive

In this second factor, we will consider the force due to the mud hose and umbilicals hanging onto the top drive.

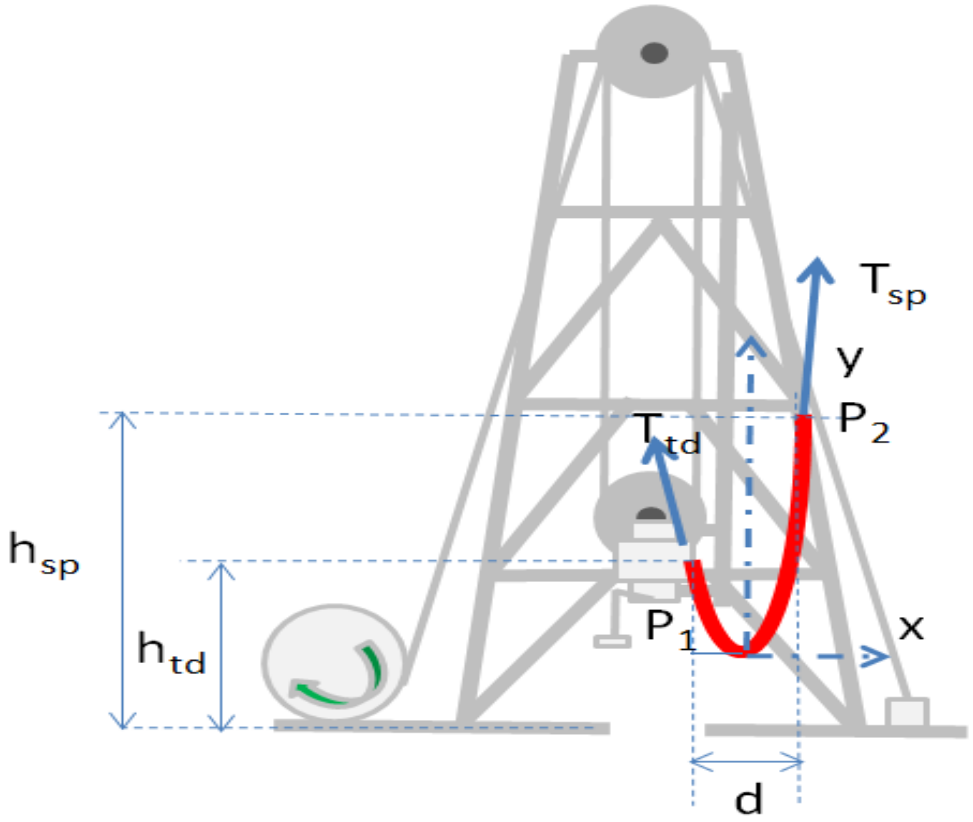

Figure 10 - A view of the effect of mud hose and top-drive umbilicals on the traveling block equipment [22]

The shape assumed by the mud hose and the umbilicals is one of a catenary curve such that;

$$y = a\ cosh\ \frac{x}{a} \qquad 4.7$$

Here, a is a parameter that defines the catenary curve

Let's represent the height relative to the drill-floor of the hanging point of the mud hose to the stand pipe by h_{sp}; the height relative to the drill floor of the hanging point of the top-drive by h_{td}, the horizontal distance between the two hanging points by *d* and the length of the mud hose by l_{mh}.

If we want to find the parameter, *a*, we can do so by solving the following equation;

$$\sqrt{l_{mh}^2 - \left(h_{td} - h_{sp}\right)^2} = 2asinh\frac{d}{2a} \qquad 4.8$$

The horizontal tension, $T_h$is the same along the entire length of the catenary curve. It is also related to the parameter *a* via the following relationship for a weighted line of linear weight $\partial_s m_{mh}$:

$$T_h = \frac{g\partial_s m_{mh}}{2a} \qquad 4.9$$

To obtain the vertical tension component at hanging points, we will determine the position of the hanging points, $P_1 = \begin{pmatrix} x_1 \\ y_2 \end{pmatrix}$ and $P_2 = \begin{pmatrix} x_2 \\ y_2 \end{pmatrix}$. This can then lead to;

$$\begin{cases} y_1 = acosh\frac{x_1}{a} \\ y_2 = acosh\frac{x_2}{a} \end{cases} \qquad 4.10$$

The above can be re-written as;

$$cosh\frac{x_1+d}{a} - cosh\frac{x_1}{a} + \frac{h_{td}-h_{sp}}{a} = 0 \qquad 4.11$$

At this point, it becomes possible to calculate the tension at the hanging points. We use the following equation;

$$T_v(x) = \frac{g\partial_s m_{mh}}{2a} sinh\frac{x}{a} \qquad 4.12$$

4.4 Effect of centrifugal force on the drill-line around the pulleys

Here, how the centrifugal force due to the rotation of the pulley affects the hook load measurement is considered. Let us denote the linear velocity of the rope that is wound around each pulley by v, the radius of the pulley is r_b and the linear weight of the rope is $\bar{\lambda}_m$.

Since the rope is in contact with the pulley, an angle θ is formed between points A and B. At the points A and B, the tension in the rope is $\vec{T}_A$ and $\vec{T}_B$ respectively. We will assume that the friction and tensions ensure that there is no slip between the rope and the pulley. This assumption will be verified to ensure that that condition is respected. We will consider friction at the level of the bearings of the pulley, $r_a$being the radius of pulley axle.

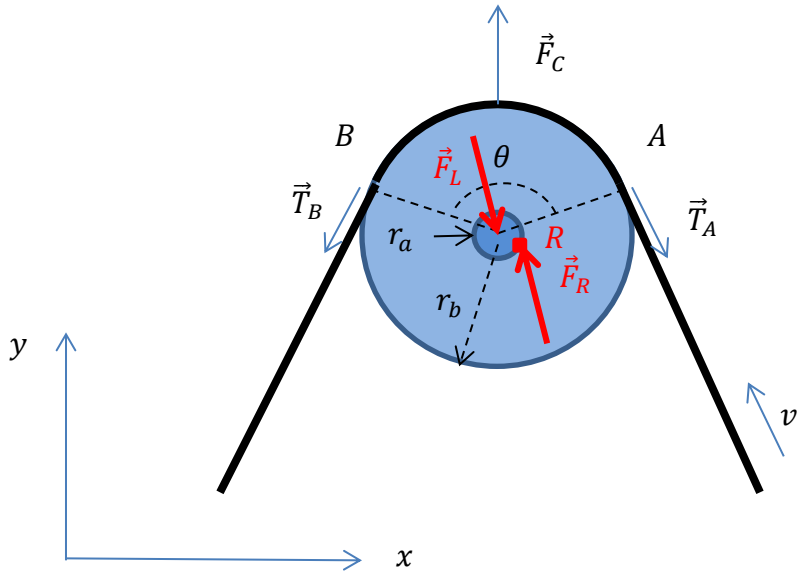

Figure 11 - Schematic view of the contact of a rope with a pulley. [22]

For considerations of uniform rotation, the balance of forces between the pulley and its axle is such that:

$$\vec{F}_L = -\vec{F}_R \tag{4.13}$$

Where $\vec{F}_L$ is the total load applied by the pulley to the axle and $\vec{F}_R$ is the reaction force between the pulley and its axle.

The total load applied by the pulley to the axle is the sum of the weight of the pulley $\vec{F}_W = -m_p g\hat{y}$ (where m_p is the mass of the pulley, g is the gravitational acceleration and $\hat{y}$ is the unit vector in the y direction), the tensions on the rope $\vec{T}_A$ and $\vec{T}_B$, and the centrifugal force applied to the element of rope that is changing direction (circular motion) $\vec{F}_C$:

$$\vec{F}_L = \vec{F}_W + \vec{T}_A + \vec{T}_B + \vec{F}_C \tag{4.14}$$

A control element of rope of length ds that is moving at angular velocity $\omega = \frac{v}{r_b}$ is subject to a centrifugal force:

$$d\vec{F}_C = \bar{\lambda}_m r_b \omega^2 \hat{r} ds \tag{4.15}$$

where $\hat{r}$ is the unit vector in the radial direction. The total centrifugal force applied on the rope around the pulley is the integral of that elementary force between A and B:

$$\vec{F}_C = \int_A^B \bar{\lambda}_m r_b \omega^2 \hat{r} ds \tag{4.16}$$

Assuming that the points A and B are symmetric compared to the y-axis, and making the change of variable $ds = r_b d\theta$, the force can be expressed in the Cartesian system as:

$$\vec{F}_C = \begin{cases} \int_{-\frac{\theta}{2}}^{\frac{\theta}{2}} \bar{\lambda}_m r_b \omega^2 r_b \sin\theta \, d\theta \\ \int_{-\frac{\theta}{2}}^{\frac{\theta}{2}} -\bar{\lambda}_m r_b \omega^2 r_b \cos\theta \, d\theta \end{cases} = \begin{cases} 0 \\ \bar{\lambda}_m r_b \omega^2 r_b \left(-\sin\left(-\frac{\theta}{2}\right) + \sin\left(\frac{\theta}{2}\right)\right) \end{cases} = 2\bar{\lambda}_m {r_b}^2 \omega^2 \sin\left(\frac{\theta}{2}\right)\hat{y} \tag{4.17}$$

We can now calculate the total load:

$$\vec{F}_L = \begin{cases} T_A \cos\left(\frac{\theta}{2}\right) - T_B \cos\left(\frac{\theta}{2}\right) \\ -m_p g + 2\bar{\lambda}_m {r_b}^2 \omega^2 \sin\left(\frac{\theta}{2}\right) - T_A \sin\left(\frac{\theta}{2}\right) - T_B \sin\left(\frac{\theta}{2}\right) \end{cases} = \begin{cases} (T_A - T_B)\cos\left(\frac{\theta}{2}\right) \\ -m_p g + \sin\left(\frac{\theta}{2}\right)\left(2\bar{\lambda}_m {r_b}^2 \omega^2 - T_A - T_B\right) \end{cases} \quad 4.18$$

Friction at the level of the axle bearings produces a moment, $\vec{M}_f$. For a uniform rotation, the sum of the moments shall be 0. $\vec{F}_W$ and $\vec{F}_C$ do not produce any moments because their direction passes through the center of rotation. So the friction moment has to be balanced by the difference of magnitude between the tensions $\vec{T}_A$ and $\vec{T}_B$:

$$\vec{M}_f = \vec{T}_A \times \vec{r}_A + \vec{T}_B \times \vec{r}_B \quad 4.19$$

where $\vec{r}_A$ is the radius vector in the direction of A and $\vec{r}_B$ is the radius vector in the direction B. All those moments are in the z-direction, *i.e.* perpendicular to the x-y plane, and therefore we can re-write this equation:

$$M_f = T_A r_b - T_B r_b = r_b(T_A - T_B) \quad 4.20$$

If we assume a Coulomb friction on the bearings, with a friction co-efficient μ_a, then the moment $\vec{M}_f$ has the magnitude:

$$\left\|\vec{M}_f\right\| = \mu_a \left\|\vec{F}_L\right\| r_a \quad 4.21$$

The friction torque works against the direction of movement. Therefore T_A and T_B are related by:

$$\pm\mu_a r_a \sqrt{\left((T_A - T_B)\cos\left(\frac{\theta}{2}\right)\right)^2 + \left(-m_p g + \sin\left(\frac{\theta}{2}\right)\left(2\bar{\lambda}_m {r_b}^2 \omega^2 - T_A - T_B\right)\right)^2} = r_b(T_A - T_B) \quad 4.22$$

where the sign in front of the frictional torque depends whether we are hoisting or lowering.

We can remove the square root by squaring the above equation:

$$\mu_a{}^2\, r_a{}^2\left(\left((T_A - T_B)\cos\left(\frac{\theta}{2}\right)\right)^2 + \left(-m_p g + \sin\left(\frac{\theta}{2}\right)\left(2\bar{\lambda}_m r_b{}^2\omega^2 - T_A - T_B\right)\right)^2\right) = r_b{}^2(T_A - T_B)^2 \quad (4.23)$$

For the particular case of $\theta = \pi$, then we obtain:

$$\mu_a{}^2\, r_a{}^2\left(-m_p g + 2\bar{\lambda}_m r_b{}^2\omega^2 - T_A - T_B\right)^2 = r_b{}^2(T_A - T_B)^2 \quad (4.24)$$

Which gives:

$$T_B = -\frac{r_b T_A + \mu_a r_a T_A - 2\bar{\lambda}_m \mu_a \omega^2 r_b{}^2 r_a + m_p g \mu_a r_a}{\mu_a r_a - r_b} \text{ or } T_B = -\frac{-r_b T_A + \mu_a r_a T_A - 2\bar{\lambda}_m \mu_a \omega^2 r_b{}^2 r_a + m_p g \mu_a r_a}{\mu_a r_a + r_b} \quad (4.25)$$

One of the solutions is hoisting and the other one is for lowering.

For a pulley in the travelling equipment, the approach is similar, but with a few changes in the orientation of forces (most notably the centrifugal force and the tensions). This results in the following equation:

$$\mu_a{}^2\, r_a{}^2\left(\left((T_A - T_B)\cos\left(\frac{\theta}{2}\right)\right)^2 + \left(-m_p g + \sin\left(\frac{\theta}{2}\right)\left(-2\bar{\lambda}_m r_b{}^2\omega^2 + T_A + T_B\right)\right)^2\right) = r_b{}^2(T_A - T_B)^2 \quad (4.26)$$

For $\theta = \pi$, this equation simplifies into:

$$\mu_a{}^2\, r_a{}^2\left(-m_p g - 2\bar{\lambda}_m r_b{}^2\omega^2 + T_A + T_B\right)^2 = r_b{}^2(T_A - T_B)^2 \quad (4.27)$$

Which gives:

$$T_B = \frac{-r_b T_A - \mu_a r_a T_A + 2\bar{\lambda}_m \mu_a \omega^2 r_b{}^2 r_a + m_p g \mu_a r_a}{\mu_a r_a - r_b} \text{ or } T_B = \frac{r_b T_A - \mu_a r_a T_A + 2\bar{\lambda}_m \mu_a \omega^2 r_b{}^2 r_a + m_p g \mu_a r_a}{\mu_a r_a + r_b} \quad (4.28)$$

Now, following our earlier assumption of a no-slip condition, we need to establish the validity of that assumption.

Let us call μ_b the friction coefficient between the rope and the pulley. For a control element of rope of length $ds = r_b d\theta$, there is a tension T on one side and a tension T+dT on the other side. At the very limit when slip could occur, we can still express the balance of forces in static conditions:

$$\begin{cases} (T + dT)\cos\left(\frac{d\theta}{2}\right) - T\cos\left(\frac{d\theta}{2}\right) - \mu_b dN = 0 \\ dN - (T + dT)\sin\left(\frac{d\theta}{2}\right) - T\sin\left(\frac{d\theta}{2}\right) = 0 \end{cases} \quad 4.29$$

where dN is the reaction force between the rope control element and the pulley. By combining the two equations we can eliminate dN:

$$\frac{dT}{d\theta}\cos\left(\frac{d\theta}{2}\right) - \mu_b\left(T + \frac{dT}{2}\right)\frac{\sin\left(\frac{d\theta}{2}\right)}{\frac{d\theta}{2}} = 0 \quad 4.30$$

By taking the limit when $d\theta$ goes to 0, we obtain:

$$\frac{dT}{d\theta} - \mu_b T = 0 \quad 4.31$$

Integrating this equation between A and B, we obtain:

$$\log\frac{T_B}{T_A} = \mu_b\theta \Leftrightarrow T_B = T_A e^{\mu_b\theta} \quad 4.32$$

By comparing T_B obtained with equation (4.25) and (4.28) with T_B obtained with equation (4.32), we can therefore determine if the slip hypothesis will be respected or not.

Let us now determine the velocity v for each pulley as a function of the traveling equipment velocity v_{tb} and the number of blocks n in the hoisting system.

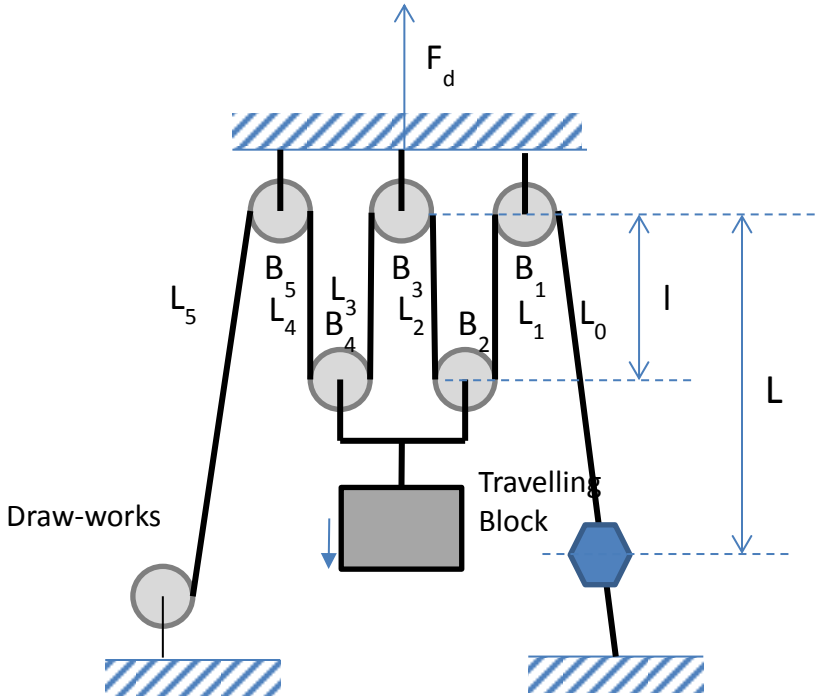

Figure 12 - A schematic of a hoisting system based on a draw-works [22]

To move the block by a distance dL, $L_0 = L$ (the length of the rope between B_1 and the anchor will not change, but the length of the rope between B_1 and B_3 needs to change by $2dL$. Similarly, the length of rope between B_3 and B_5 needs to change by $4dL$ and therefore we obtain the general relationship that:

$$\forall i \in [0, \frac{n}{2}]\ v_{2i} = 2iv_{tb}\ and\ v_{2i+1} = 2iv_{tb} \tag{4.33}$$

where v_i is the velocity of the rope at the level of the block i.

4.5 Sensitivity analysis of model

In order to analyze the theoretically model in terms of trend, an Excel program was written and each parameter adjusted to find which parameters greatly influence the hook load readings. This was also done to analyze the trend between the theoretical model and the experimental data; to ensure a strong relation between experiment and the model equation which have been developed. This is called sensitivity analysis.

In this sensitivity analysis, to investigate the impact of each parameter, all other parameters are held constant. This is to ensure that the full impact of the parameter in question is felt on the model.

4.5.1 Changes in velocity

For this simulation, the block velocity is allowed to vary from 0,02 to 0,1m/s, the hook load changes shows insignificant. Table 1 and Figure 14 shows the % change hook load the given velocity variation. During the experimental test (chapter 5), the effect of velocity change was not studied because the experimental setup did not contain a velocity control unit.

Table 1: Percentage change in hook load due to changes in velocity

Velocity values	% change
0.02	0,054832198
0.04	0,109829388
0.06	0,109828586
0.08	0,109827884
0.1	0,109826981

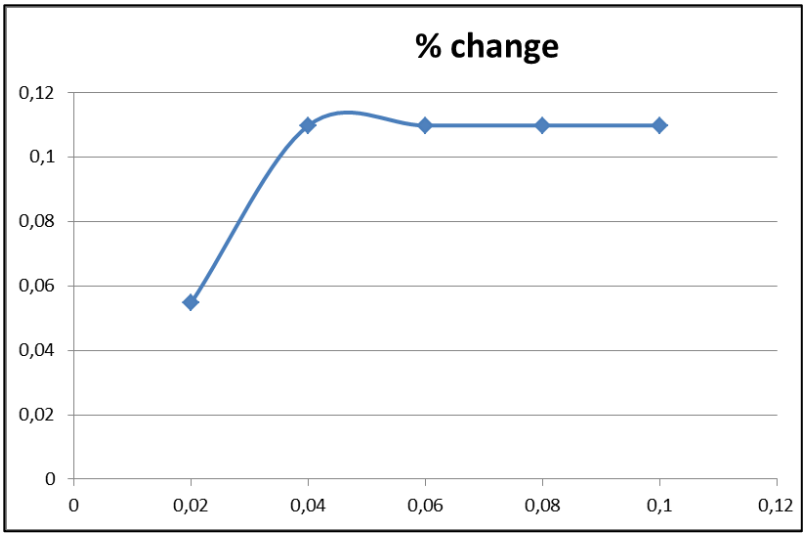

Figure 13: Graph displaying the percentage changes in hook load depending on velocity

This approach was used to investigate the effect of changing velocity on the hook load readings. From the graph, it can be deduced that the velocity has very minimal effect on the overall hook load reading that is registered at the dead-end. From the model developed, the angular velocity, which is linearly proportional to the linear velocity, ie, $v = r\omega$. Therefore investigating the impact of the linear velocity is a way to determine how much the angular velocity influences the

hook load reading. From the graph, there is a sharp rise between v = 0.02m/s and 0.04m/s. Beyond v = 0.04m/s, the graph flattens out which indicates a no net change in the value of the velocity.

Between velocity values of v = 0.04m/s and 0.06m/s, there is a slight reduction. This sensitivity analysis proves that at higher velocity, we have lower hook load readings, and vice versa. This observation is further re-iterated by an experiment carried out at NTNU where they got the following figure 14.

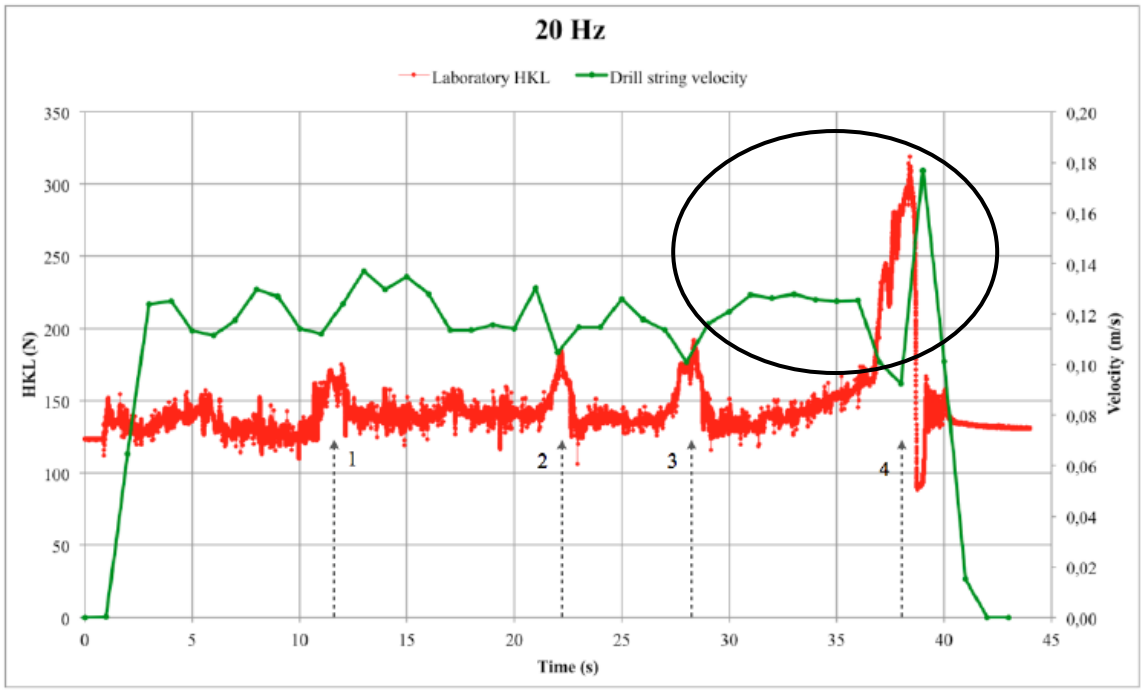

Figure 14 - Graph indicating the relationship between hook load and velocity with time

The figure above is a plot of velocity and hook load against time. From the figure, it can be deduced from the part with an oval shape that at lower velocity, a higher hook load reading is observed, and at high velocity, a lower hook load is observed.

4.5.2 Effect of friction

The effect of friction is investigated with the friction co-efficient, since friction, $\boldsymbol{f = \mu R}$, where μ is friction co-efficient and is linearly proportional to the friction. Table 2 and figure 15 show the simulation result on percentage change in hook load due to changes in friction.

Table 2: Percentage change in hook load due to changes in friction

Friction	% change
0,02	0,14658635
0,04	0,29435484
0,06	0,44331984
0,08	0,59349593
0,1	0,74489796

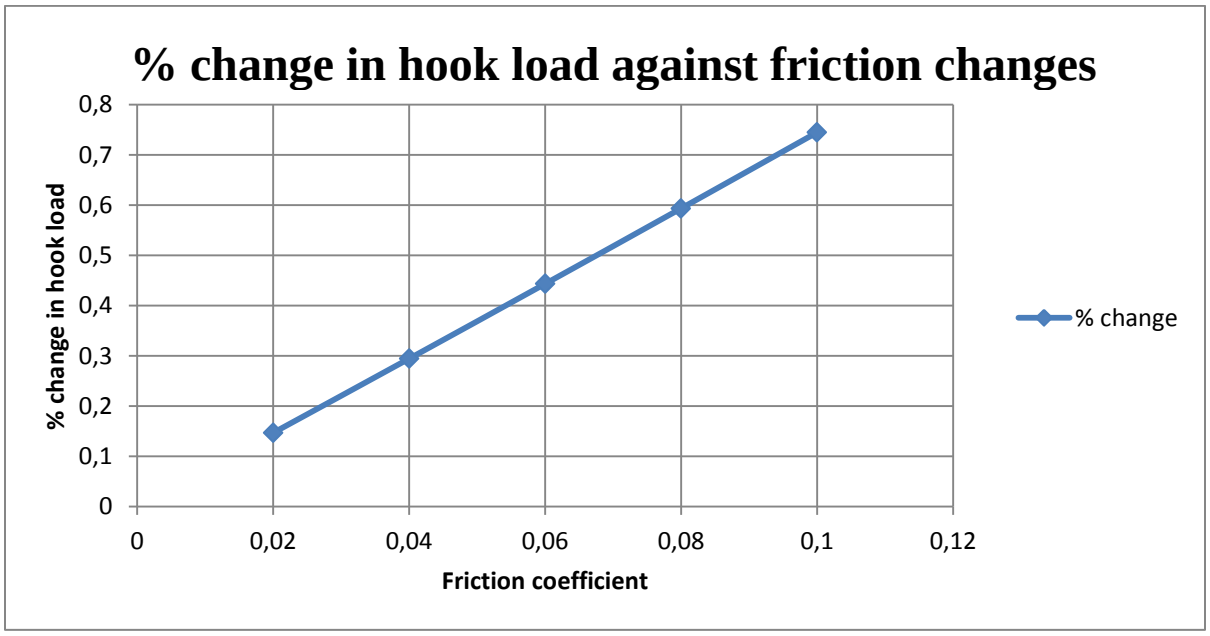

Figure 15 - Graph of the percentage change in hook load with respect to changes in friction

Friction has a rather negative, yet increasing effect on the hook load reading. From the model developed, i.e.

$$T_B = \frac{-r_b T_A - \mu_a r_a T_A + 2\bar{\lambda}_m \mu_a \omega^2 {r_b}^2 r_a + m_p g \mu_a r_a}{\mu_a r_a - r_b} \text{ or } T_B = \frac{r_b T_A - \mu_a r_a T_A + 2\bar{\lambda}_m \mu_a \omega^2 {r_b}^2 r_a + m_p g \mu_a r_a}{\mu_a r_a + r_b},$$

the higher the co-efficient of friction value, the less the tension, T_B recorded at the hook load sensor. Increases in friction could be due to high velocity, material of drill line, etc. The higher the velocity of the travelling equipment, the higher the friction generated, and hence, the lower the hook load reading.

5 Hook load experiments

In order to validate the model that has been developed, an experimental set up was built in the shape of the rig to take hook load measurements under several conditions and factors. These measurements will then be used to match the results from the model to ascertain the model's accuracy.

5.1 The experimental setup

The experimental setup was built with a pulley system with five pulleys in the crown block and four in the travelling block. These separate set of pulleys are linked with a low weight string; which will be later varied to determine the effect of the weight of the drill line on the hook load readings.

The experimental setup consists of the following components;

a. Crown block
b. Load cells on the crown block
c. Pulleys
d. Electronic weight indicator
e. Electronic velocity measuring device
f. Weights of various masses at the travelling block
g. A main and supporting metallic frame to support the structure
h. A winch to serve as draw works
i. A voltmeter reader to record the hook load
j. A computer setup to automatically record data

5.1.1 Experimental procedure

Various procedures were employed in the experiment to determine the effect of different factors on the hook load measurements. Below are a few of them;

a. Different drill lines of various weights were used to determine if the weight of the drill line had any significant effect on the hook load reading.
b. Various weights were added to the travelling block to ascertain the impact of different weights on the hook load measurements.
c. The experimental setup was run at constant speed (no acceleration), and at different speeds to evaluate the impact of speed on the hook load readings.
d. To investigate the effect of each pulley's efficiency, the pulley arrangements were altered in different configurations.

In order to ascertain that the hook load readings are not necessarily dependent on the arrangement of the pulley, the pulleys were numbered and their positions altered after each experiment. Results were recorded and the respective parameters determined.

5.1.2 Investigation of various model parameters

From the model built, several factors are considered as having likely effect on the overall hook load reading at the dead line. As such, these factors were investigated to ascertain what level of impact they have on the hook load readings.

5.1.2.1 Effect of mud hose tension

To be able to determine the effect of the mud hose tension and other umbilicals, a chain of a known weight was hanged on the frame of the experimental rig setup and the traveling block. This chain was intact as the travelling block made hoisting and lowering runs. The results were recorded and will be reported in subsequent sections.

5.1.2.2 Effect of dolly retraction

In the development of the model, retracting the dolly was seen to have an effect on the overall hook load reading. When the traveling block is retracted and spun into the crown block and back,

the hook load readings could be altered. To investigate this, the traveling block is attached to a side-structure designed to serve as a dolly.

The traveling block is then hoisted and lowered while it is attached to the dolly-like structure. Measurements of the hook load were taken and analysed.

5.1.2.3 Effect of weight of drill line

In the model, one of the factors that featured prominently was the weight per unit length of the drill line. Since different drill lines have different weights per unit length, it means each drill line will have some effect on the hook load reading. This was also investigated with the use of two different drill lines. The measurements of the resulting hook load were taken and analysed.

5.2 Error reporting

Like most, if not all experiments, this experiment is not devoid of possible sources of errors. Some of the possible sources of error are;

a. Source of voltage

To be able to record hook load readings on the computer, the system was connected to a voltmeter which measures the signal in the dead line in the form of millivolts. To be able to measure the signal, the dead line sensor is powered by a dry cell battery. This battery begins at a very high voltage level and declines with time.

This decline has some negative influence on the sensitivity of the battery to transferring signals from the dead line to the volt meter.

b. Oscillations in the set up

During hoisting and lowering, which is enabled by the turning of the winch, there are “disturbances” introduced into the system. This, in turn, is transferred to the pulleys and drill line. This could be visibly seen as the lines and pulleys are somewhat unstable. This instability leads to the introduction of a fluctuating effect in the readings at the dead line.

c. Human error

Since human operates the setup, it is inevitable that errors could be introduced into the setup and possibly, the readings. To a large extent, it was aimed to operate the system at a fairly constant speed. But the absence of a speed reader meant one would measure the speed manually; which is quite inaccurate.

5.3 Mitigating experimental errors

Knowing these errors is not enough. Mitigating them is therefore the way to control their possible effects on the experimental readings. Mitigating them becomes even more crucial since they could add up and introduce large margins of deviation from what is actually meant to be.

5.3.1 Source of voltage

Since the whole experiment literally depended on the readings at the dead line, and as such the dry cell which transferred signals from the dead line to the volt meter and onward to the computer, it was crucial to monitor the voltage level of the dry cell. When the starting voltage fell below -0.45, it was necessary to replace the dry cell in order to ensure that every possible signal is tracked and recorded.

This ensured a fairly uniform pattern of the values that were recorded.

5.3.2 Oscillations in the setup

Since these oscillations were inevitable under no condition, it was ensured that the winch was wound at a fairly low velocity. Of course at higher velocities, the whole experimental setup experienced vibrations due to the up and down movement of the winch. However at lower speeds, the oscillations observed were minimal and could be entertained.

5.3.3 Human errors

To mitigate any human sources of errors, the data measurement procedure was automated and done with the help of software. Also, each experiment was carried out five times to ensure accuracy. These five experiments are then averaged out for interpretation.

Figure 16 below shows a photographic picture of the experimental set up.

Figure 16 – Photographic picture of experimental set up

5.4 Experimental Data Reporting and Analysis

In the experiment that was carried out, the following were investigated to ascertain how much they affected the hook load reading;

a. The linear weight of the drill line
b. The hook load when the dolly is retracted
c. The effect of mud hose and other umbilicals hanging from the top onto the traveling block.

In order to ensure accuracy, experiments were conducted for two-pulley, three-pulley, and four-pulley travelling block systems. This was to serve as a check to the accuracy of results.

5.4.1 Three Lines

5.4.1.1-5kg weight

5.4.1.1.1 Efficiency during 5kg weight hoisting

It was noticed that for an accurate analysis, it was important to determine the efficiency of each system. To evaluate the efficiency, the following parameters were inputted into an Excel program with a Newton-Raphson formular;

a. Weight of travelling block
b. Mass of weight
c. Measurement at the dead line
d. Number of lines

From the graph below, it can be observed that the efficiency for a 5kg-mass increased from a value below 90.15% and converges at a value slightly greater than 90.82%. The interesting observation that was made was that, each lowering and hoisting had a different efficiency.

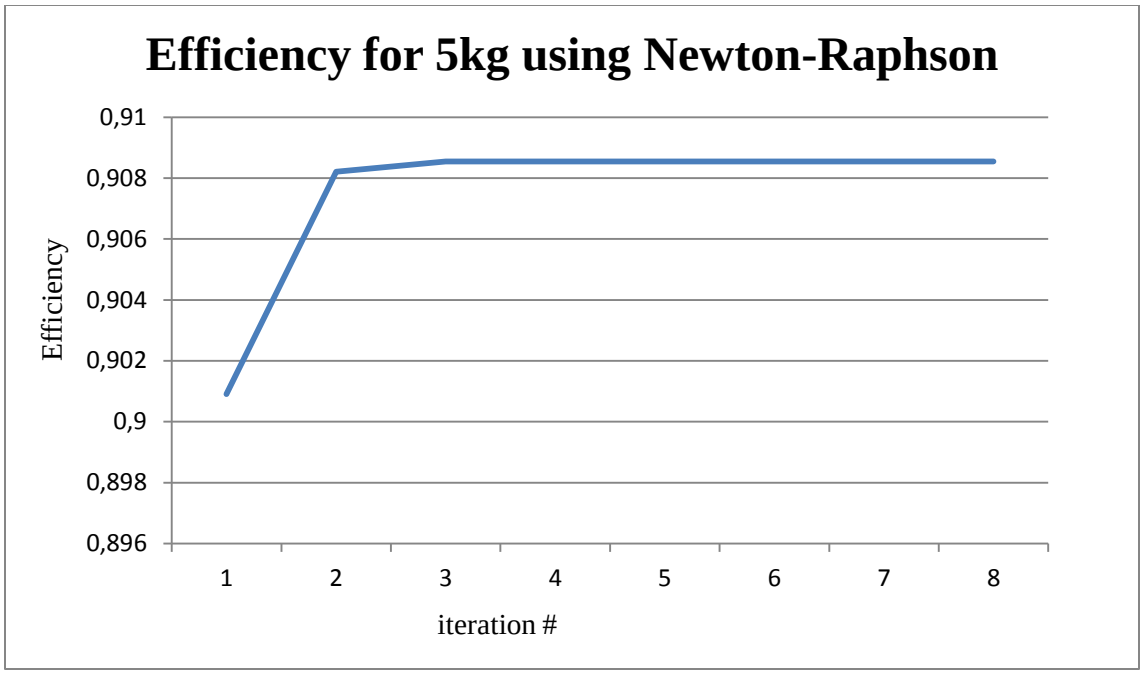

Figure 17 - Plot of efficiency during hoisting for a 5kg-mass using Newton-Raphson method

This is understandable because for each mass, say 5kg, different readings are recorded at the dead line when hoisting and lowering; which attests to the observation that each process, hoisting and lowering, had different efficiency values.

5.4.1.1.2 Efficiency during 5kg weight lowering

As was earlier stated, different efficiency values were recorded for the same weight of mass, depending on whether we are hoisting or lowering. The graph below also shows the plot of efficiency values that were iterated using the Newton-Raphson method.

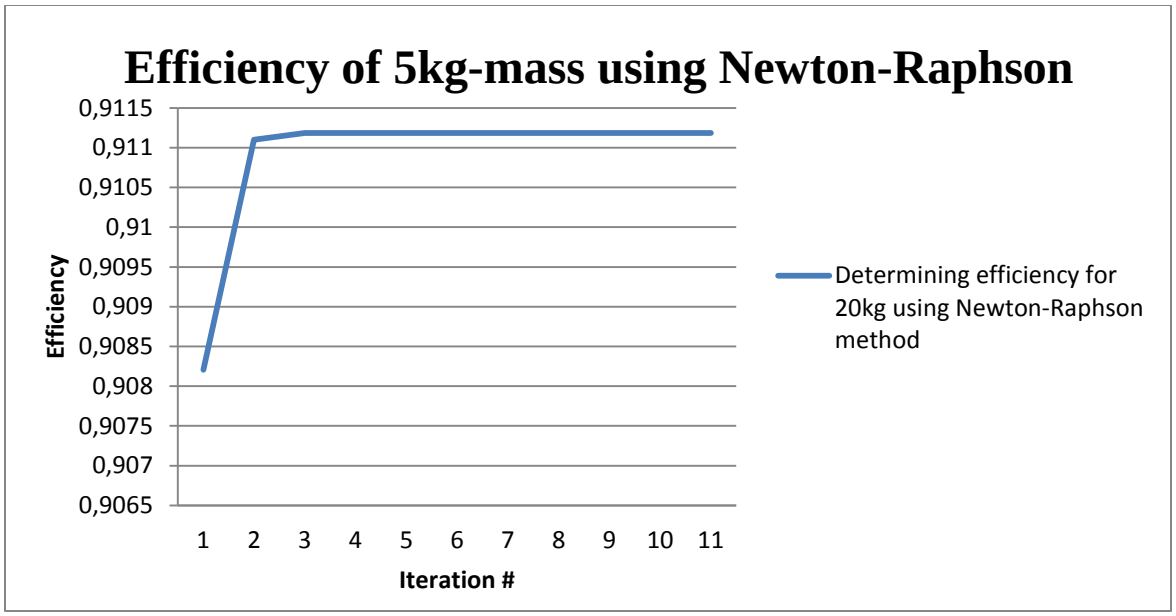

Figure 18 - Plot of efficiency vs. number of iteration during lowering for a 5kg-mass using Newton-Raphson

In this instance, it is clearly observed that the efficiency values ranged from a little less than 93.5% and converges at a little greater than 96%. That is to say, for a lowering process, we have higher efficiency than for a hoisting process of the same weight. This is a common thread in all other weights to be observed.

5.4.1.1.3 Analysis for 5kg hoisting

In order to ensure more accuracy and reduce errors, five repeatable experiments were carried out for each weight. Then the average of these values is taken for analysis. From the above figure, it is observed that during hoisting, the weight is gradually lifted from the floor through to the top. The hook load is measured for each position and recorded.

This is the plot of position on the horizontal axis, and experimentally measured hook load (kg) for five experiments during the hoisting of a 5kg weight.

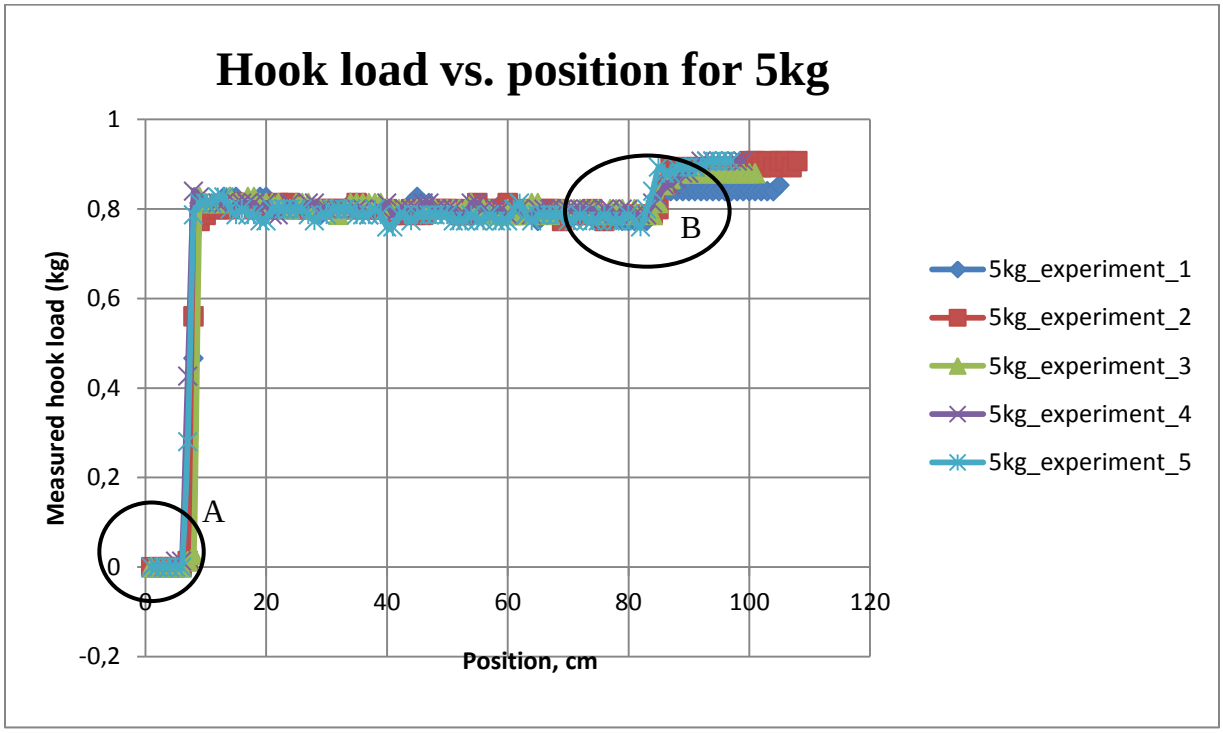

Figure 19 - Plot of hook load against position for five different experiments for 5kg

At the bottom of the figure labelled 'A', it can be observed that there is a sharp rise from 0 (zero) to about 0.8. This occurred when the weight was lying down flat and the lines are slack. Upon hoisting, the weight immediately lifts from the ground, where the reading at the dead line sensor responds to the immediate tautness in the line.

As the hoisting process continues, the readings are fairly constant until the winch is stopped at the designated location for reading. During this sudden stop, the readings increase gently which is attributed to rise observed at point 'B'.

5.4.1.1.4 Analysis of 5kg during lowering

Figure 20 indicates the plot of position against experimentally measured hook load for 5kg during lowering. Lowering follows right after hoisting. Thus it will be seen that the starting value of the lowering process is where the hoisting ended. In other words, the lowering began where the hoisting left off. This is also observed by Luke and Juvkam. It can therefore be observed that

the graph above begins from about 0.9kg and rises to between 1.2 and 1.4kg. A sharp decline is however observed and the tail-end of the graph.

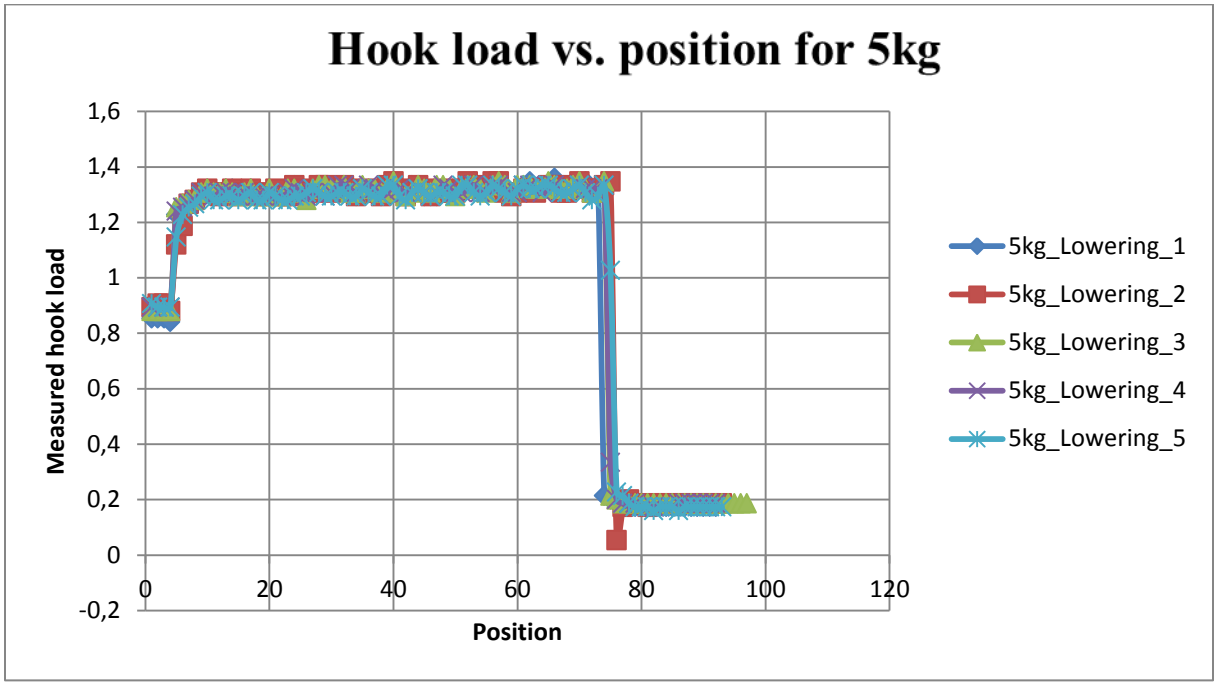

Figure 20 - Plot of hook load against position for five different experiments for 5kg

This sharp decline happens when the weight is landed to the ground. Thus the taut nature of the lines and suddenly brought to a minimal value of about 02.kg. lowering is therefore an opposite process to hoisting.

5.4.2 -20kg weight (Three Lines)

5.4.2.1 Efficiency during 20kg weight hoisting

In the case of the 20kg weight, a similar process of the Newton-Raphson method was employed to determine the efficiency. From the figure above, it can be seen that the efficiency values begin from a value slightly less than 89.8%. It then converges at a value of about 90.5%. this is as indicated in figure 21 where the efficiency is plotted against the position during the hoisting of a 20kg-mass.

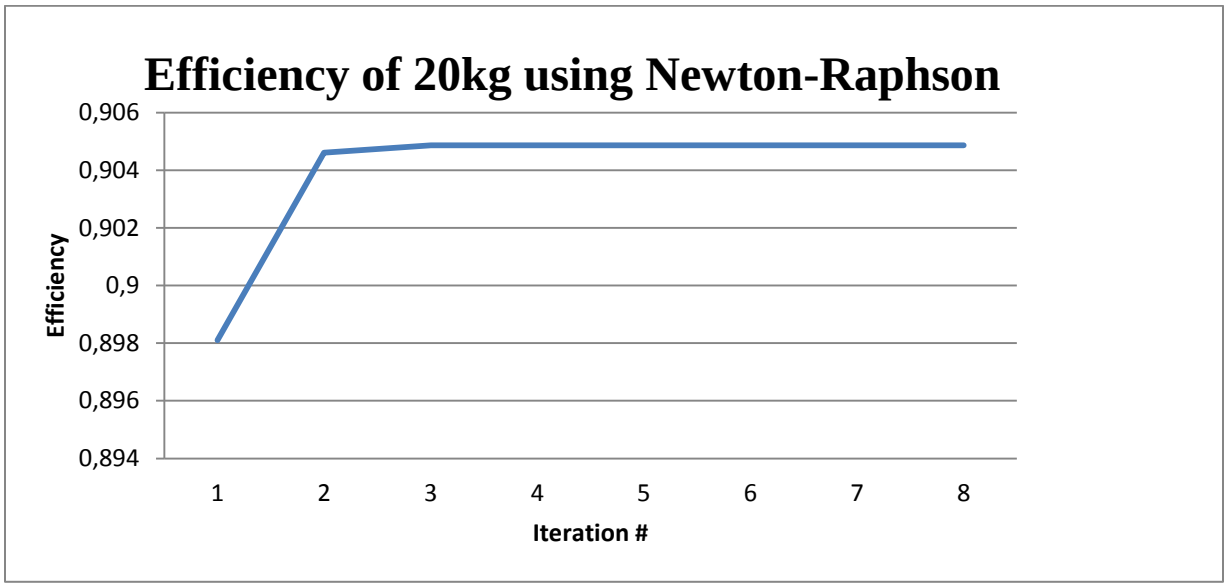

Figure 21 - Plot of efficiency vs. position during hoisting for a 20kg-mass using Newton-Raphson

5.4.2.2 Efficiency for 20kg during lowering

Like was observed in the case of the 5kg weight, the efficiency for a 20kg weight during lowering is greater than during hoisting. In the figure 22 below, the efficiency value begins from about 94.4% and converges at 98.4%.

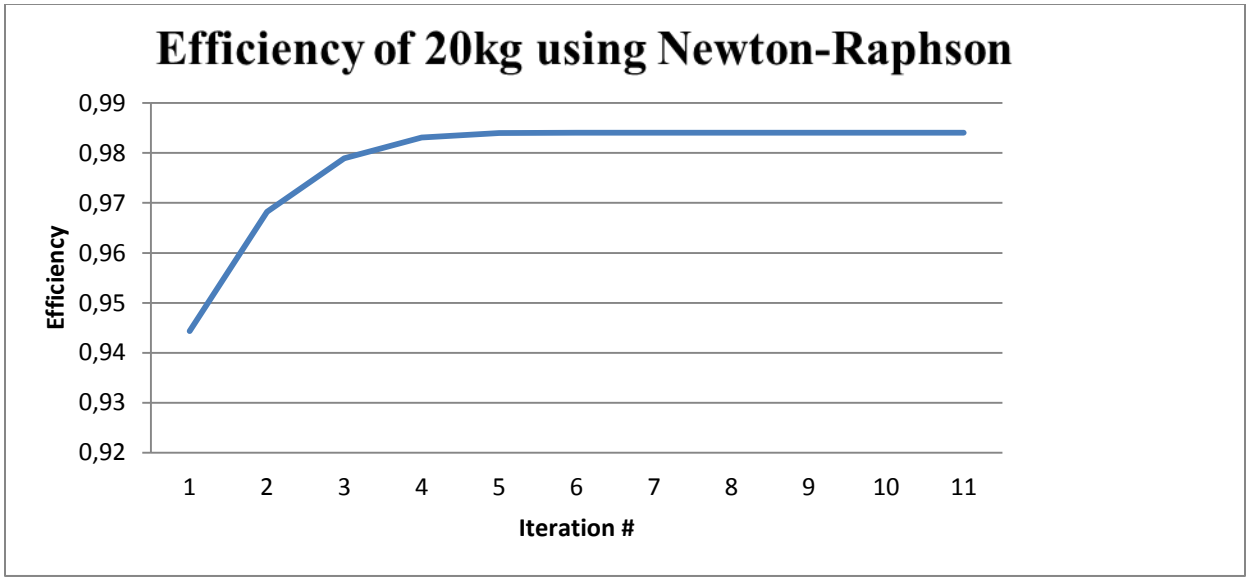

Figure 22 - Plot of efficiency during lowering for a 20kg-mass using Newton-Raphson

5.4.2.3 Analysis for 20kg during hoisting

During the process of hoisting with a 20kg weight, the figure above was obtained when the results were plotted with hook load against position. It is observed that there is a sharp increase in the hook load reading from 0.0kg to about 2.75kg. From then on, there is a fairly constant recording of values till at a gradual increase was observed which took the values a bit higher than 2.75kg.

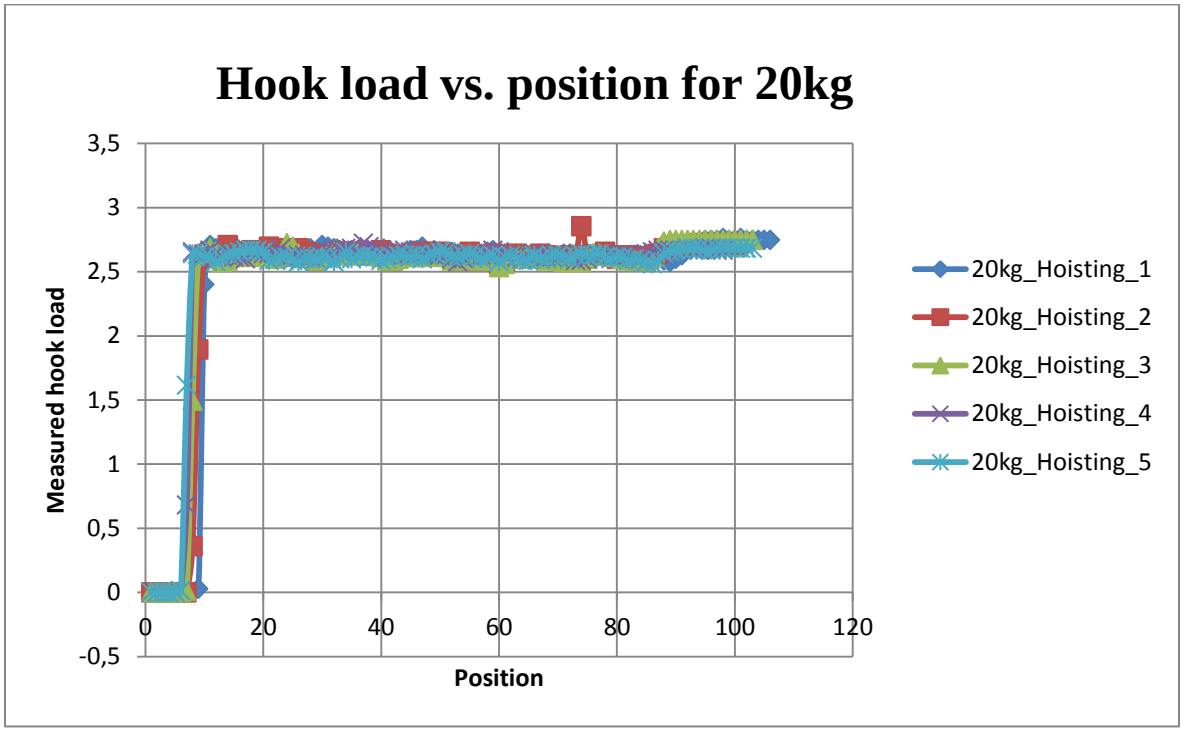

Figure 23 - Plot of hook load against position for five different experiments for 20kg

This sharp increase was due to the sudden tautness that is experienced in the line when the weight is just lifted off the ground. As the hoisting continues, there is a generally constant record of values till when it is stopped. This sudden stop also brings about a slight increase as is observed in the figure.

It is however interesting to state that for this particular experiment, all five different experiments of the same weight were insignificantly different, i.e. they were more uniform and close to one another. This attests to the level of accuracy in the figures recorded.

5.4.2.4 Analysis for 20kg during lowering

The lowering for 20kg began from about 2.75kg, where the hoisting left off; this is an increase to about 3.75kg. This value is fairly maintained through till at a position at 80 where there is a sharp decrease to about 0.25kg.

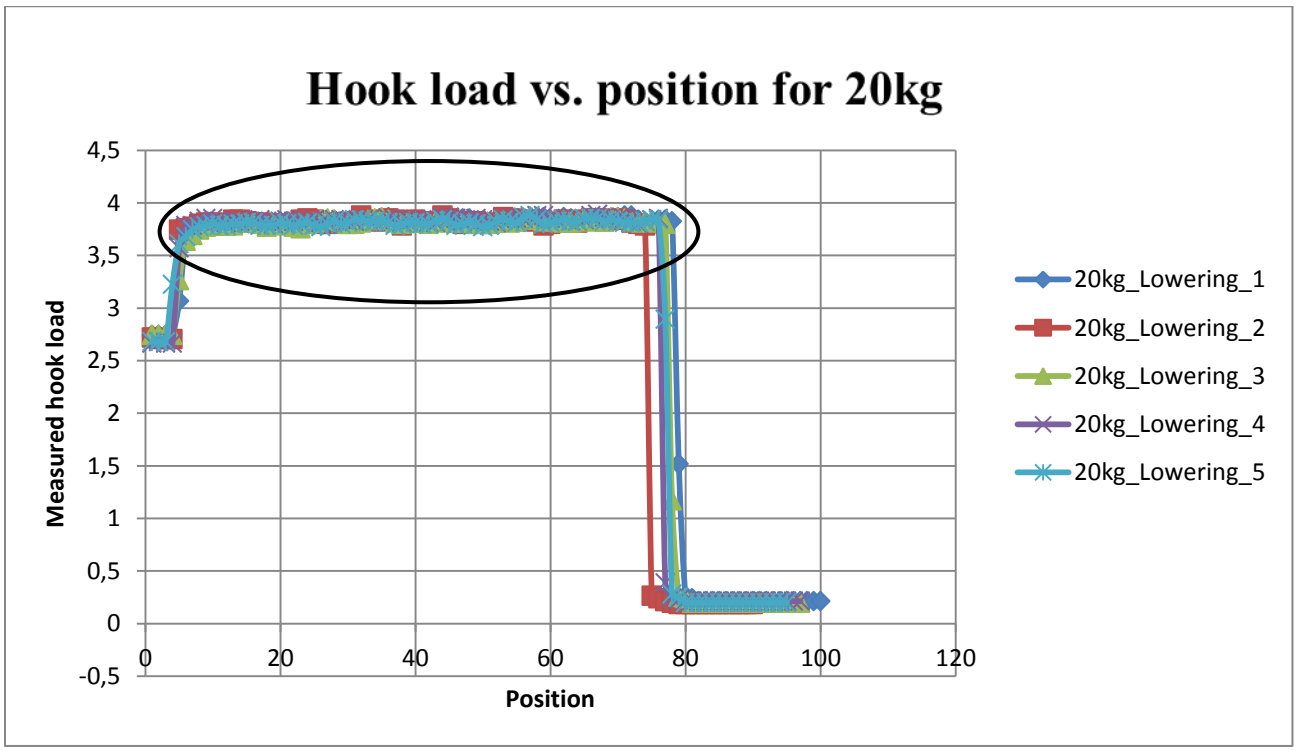

Figure 24 - Plot of hook load against position for five different experiments for 20kg

It should be understood that this sudden drop in the hook load at the tail-end of the graph is due to the drop of the weight on the floor. The drop signifies a close-to-zero tension in the lines as the tautness of the line is reduced and make slack. This is the cause of the sudden drop in hook load reading.

As such, for the sake of any analysis, the middle portion of the graph, which is indicated with the oval shape, is relevant. The earlier and latter portions of the graph are not very representative of the process. This is true for all other lowering and hoisting processes, and irrespective of the weight.

5.4.3 40kg weight (Three Lines)

5.4.3.1 Efficiency for 40kg during hoisting

Like for the previous weights that have been discussed, determining the efficiency for the 40 kg weight during hoisting was done with the help of the Newton-Raphson method. In this method, an average value of the hook load readings taken in the middle portion of the graph was used.

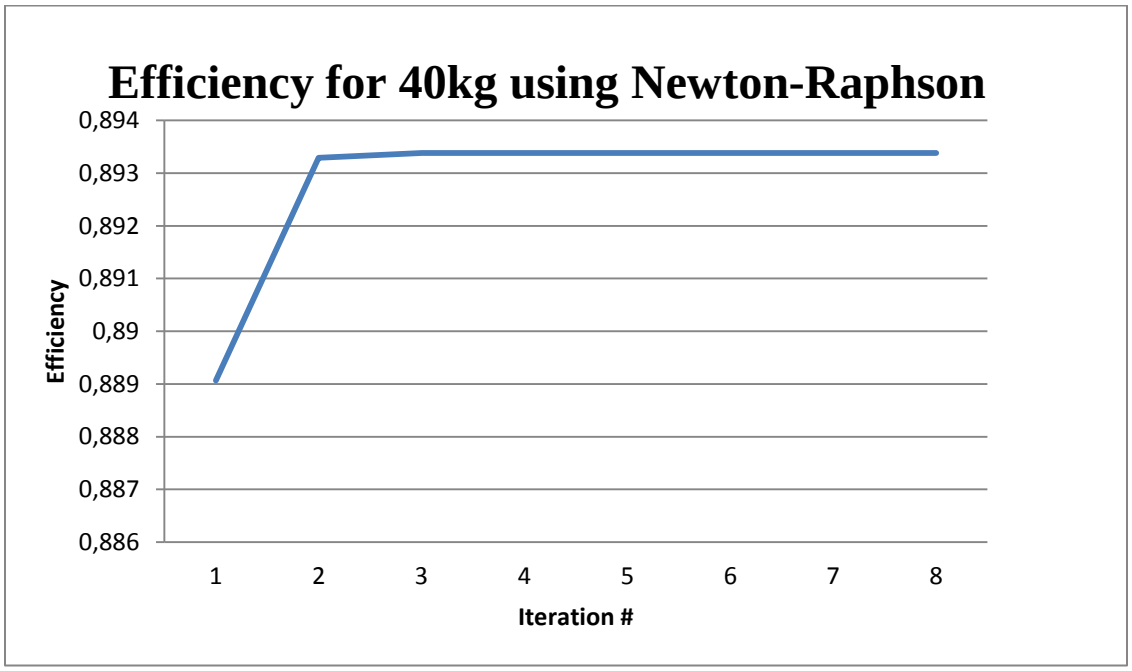

Figure 25 - Plot of efficiency during lowering for a 40kg-mass using Newton-Raphson

As is seen from the figure above, the efficiency value begins from 88.9% and converges at about 89.34%. For calculation purposes, a representative value of 89.34% is appropriate for consistency and accuracy. This is because majority of the hook load readings have their individual efficiencies converging at 89.34%.

5.4.3.2 Efficiency for 40kg during lowering

For the efficiency of 40kg during lowering, the efficiency value begins from about 94.3% and converges at about 98.1%. This range of values is greater than what was obtained in the case of hoisting. This follows in a similar trend as the earlier weights that were observed.

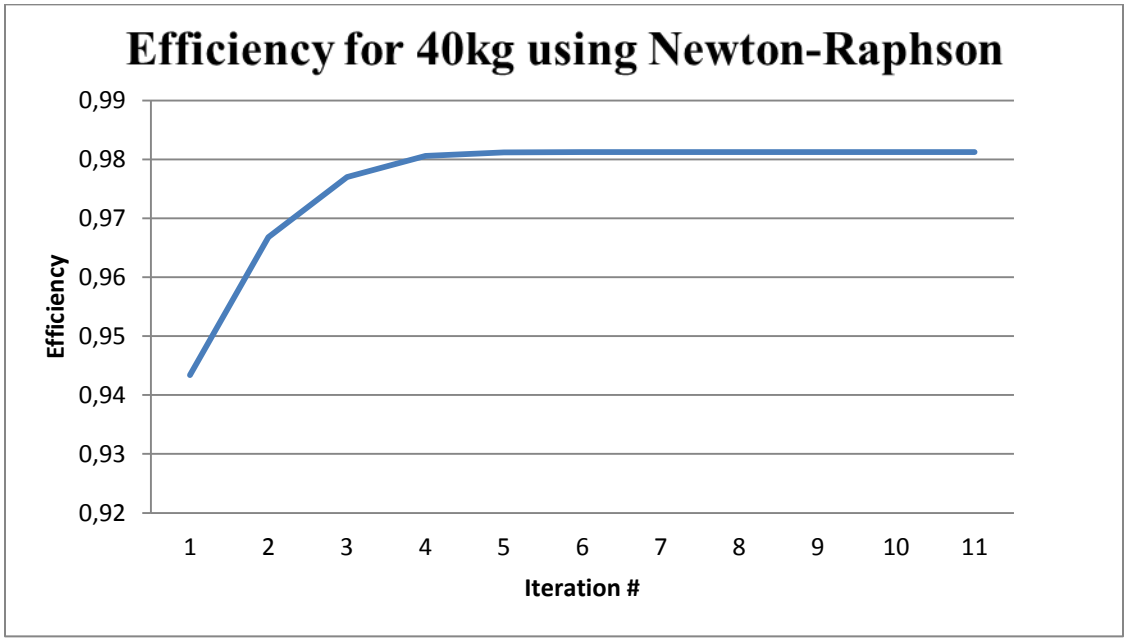

Figure 26 - Plot of efficiency vs. position during lowering for a 40kg-mass using Newton-Raphson

5.4.3.3 Analysis for 40kg during hoisting

Figure 27 shows experimentally measured hook load data against position for five different experiments for 40kg during hoisting

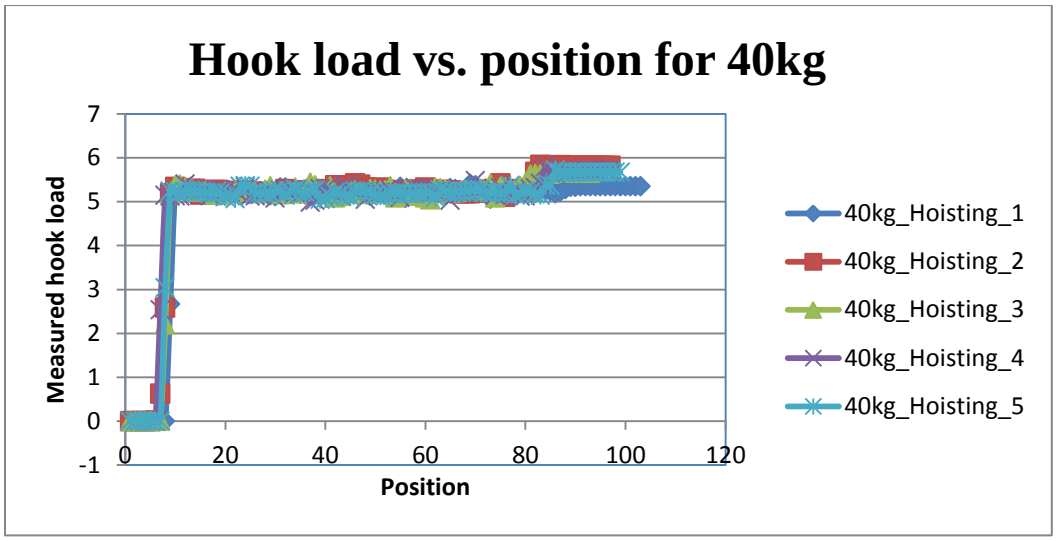

Figure 27 - Plot of hook load against position for five different experiments for 40kg

In a similar fashion as was observed for the prior weights of 5kg and 20kg, the figure for the hoisting of 40kg weight from the ground to a position close to the crown block depicts a start from 0kg where the weight is on the floor. A sharp increase in hook load is again observed from 0kg to about 5.4kg. This value remains fairly constant for all the five different experiments. The hook load reading, however, increases slightly above the 5.4kg.

5.4.3.4 Analysis for 40kg during lowering

Consistently in a similar fashion as has been seen for the previous weights, the graph for the lowering is begins from the value from where the hoisting was halted. A general increase from about 5.5kg to about 7.3kg is recorded. This value is held fairly with little fluctuations until it finally drops sharply to a value close to 0kg.

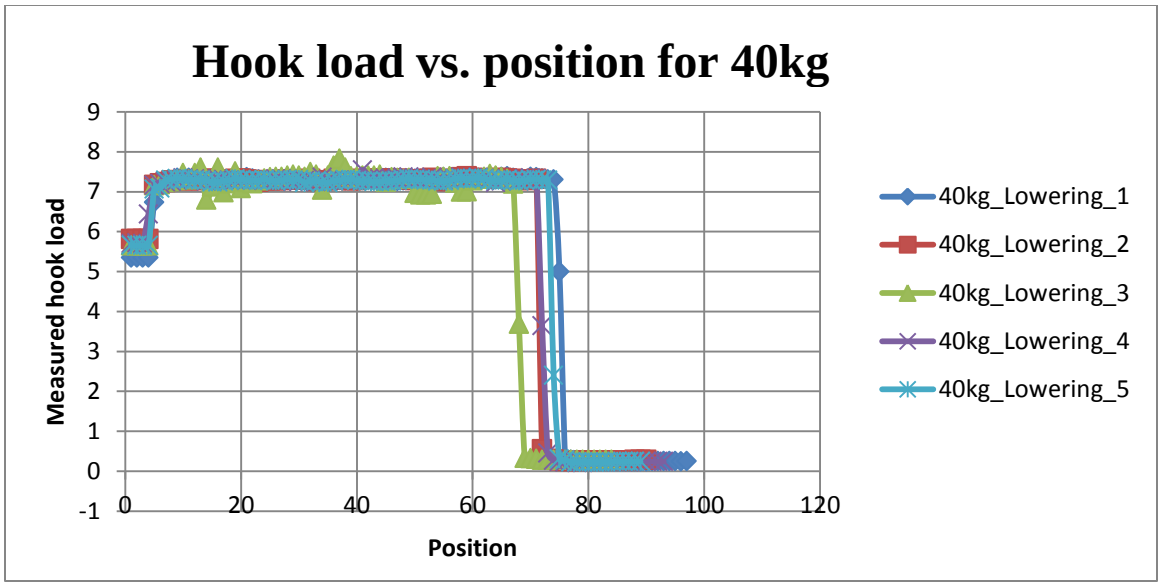

Figure 28 - Plot of hook load against position for five different experiments for 40kg

5.4.2 Two Lines

5.4.2.1 5kg weight

5.4.2.1.1 Efficiency for 5kg hoisting

Figure 29 indicates a plot of the efficiency vs. position for a mass of 5kg during lowering.

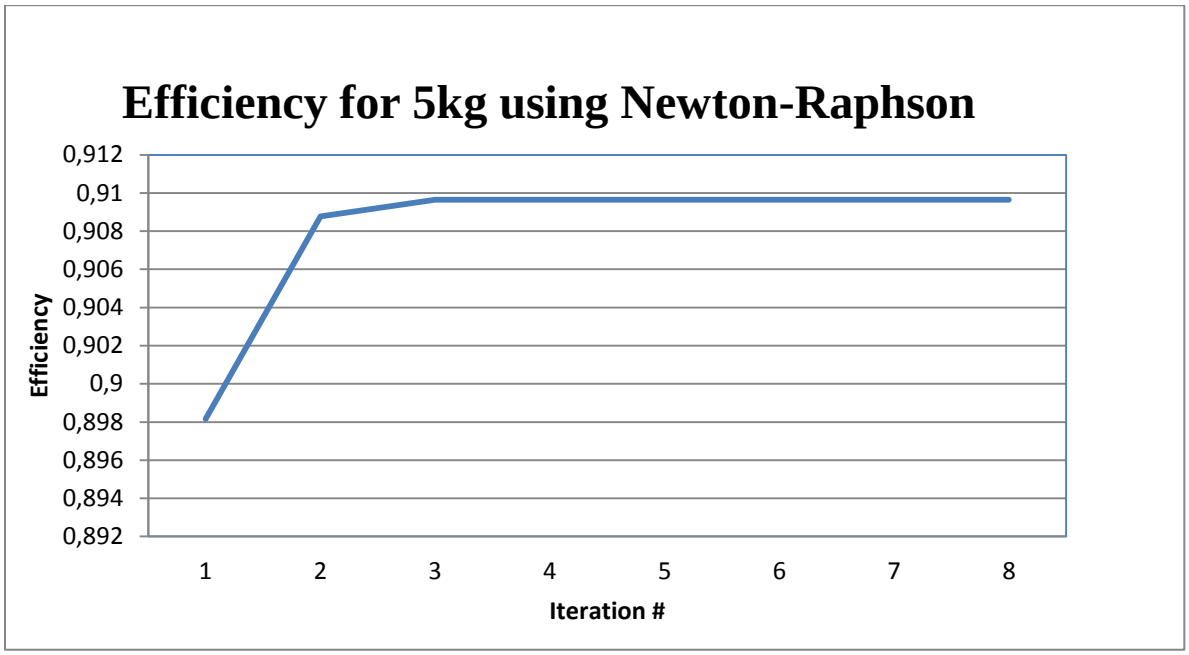

Figure 29 - Plot of efficiency vs. position during lowering for a 5kg-mass using Newton-Raphson method

From the Newton-Raphson method, the efficiency is determined for a 2-pulley 5kg weight during hoisting. It can be seen from the figure that the efficiency begins from a value of about 89.75% and converges at 91%. Now, this is greater than what was observed for a 3-pulley 5kg weight during hoisting.

With reference to the 3-pulley 5kg graph for hoisting, the efficiency increased from a value below 83.81% and converges at a value slightly greater than 83.85%. Further analysis will attempt to draw a link between the number of lines and the observed experimental efficiency.

5.4.2.1.2 Efficiency for 5kg during lowering

In the graph of efficiency for randomly selected hook load values for 5kg during lowering, the above depicts that the efficiency values range from about 62.2% and converges at 80%.

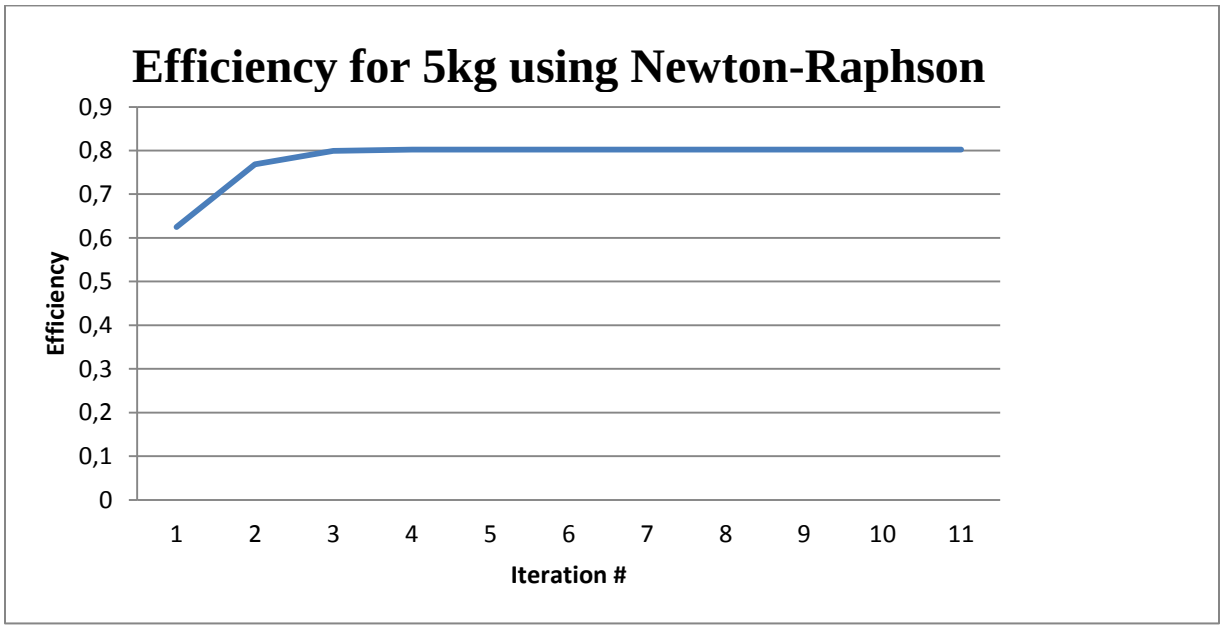

Figure 30 - Plot of efficiency vs. position during lowering for a 5kg-mass using Newton-Raphson method

Upon comparison, the efficiency values for 5kg during lower for a 3-pulley system at the travelling block ranged from a little less than 93.5% and converge at a little greater than 96%. This also shows a good observation. The efficiency value for the 2-pulley system at the travelling block is recording less value than for the three-pulley system.

5.4.2.1.3 Analysis for 5kg during hoisting

Figure 31 indicates the plot of hook load against position for a 5kg mass during the process of hoisting.

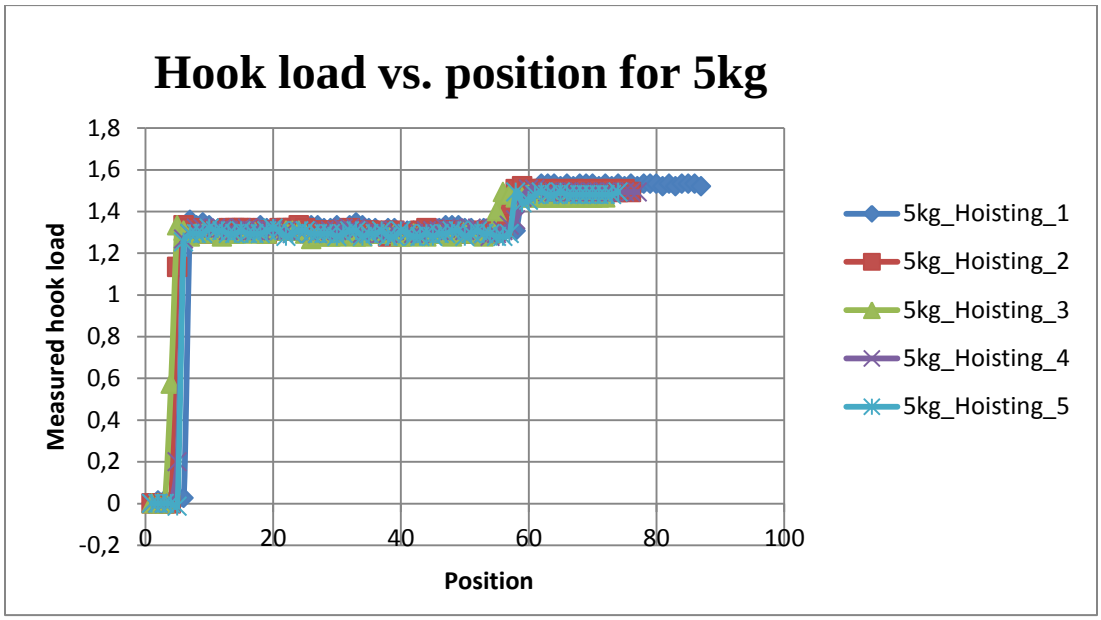

Figure 31 - Plot of hook load against position for five different experiments for 5kg

For the hoisting process of a weight of 5kg for a 2-pulley system at the travelling block, it is observed from the figure that from a starting value of 0kg, there is a sharp increase in the hook load to about 1.3kg. This is maintained through till at about the 60th position where a gentle increase is again observed from 1.3 to about 1.5kg.

5.4.2.1.4 Analysis for 5kg during lowering

From the hoisting of the 5kg weight, a hook load value of 1.5kg was finally recorded. Since the lowering follows after the hoisting, the values here begin from just where the hoisting left off; that is the previous hoisting history.

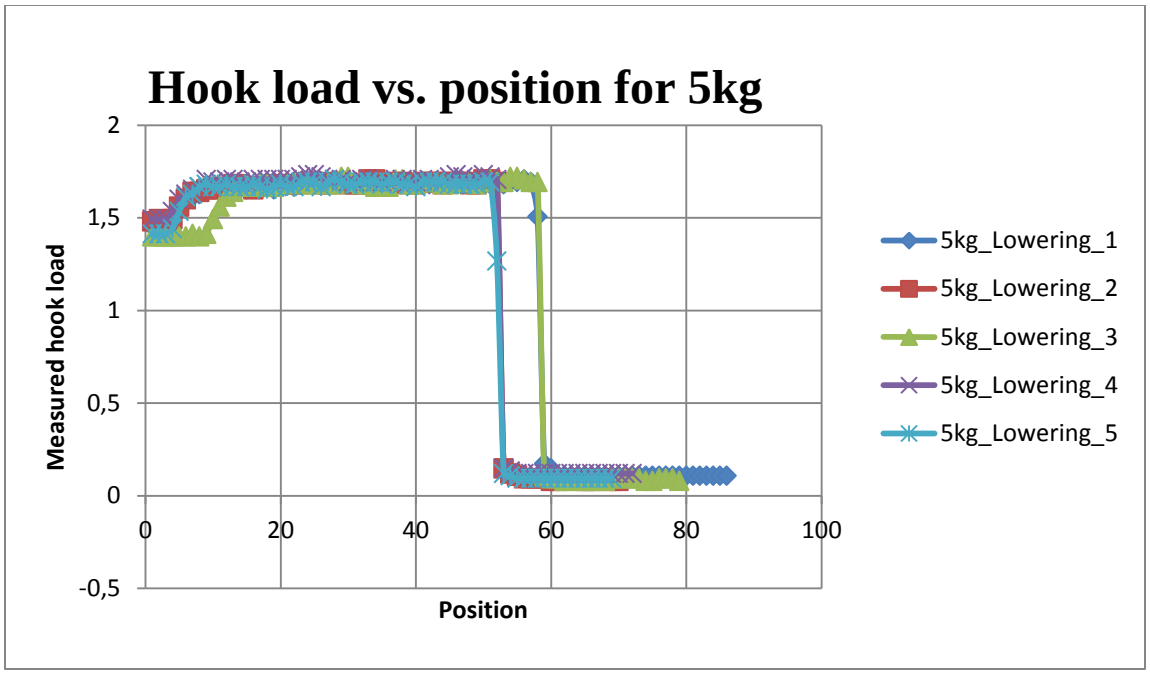

Figure 32 - Plot of hook load against position for five different experiments for 5kg

From the hoisting of the 5kg weight, a hook load value of 1.5kg was finally recorded. Since the lowering follows after the hoisting, the values here begin from just where the hoisting left off; that is the previous hoisting history.

The values for the lowering begin averagely from 1.5kg and rises gently to about 1.54kg. This is maintained until the block is finally dropped to the ground where a steep decline is observed at a position between 40 and 60.

5.4.2.2 20kg weight

5.4.2.2.1 Efficiency for 20kg during hoisting

Figure 33 shows a plot of efficiency using the Newton-Raphson iteration method during the lowering of a 20kg-mass.

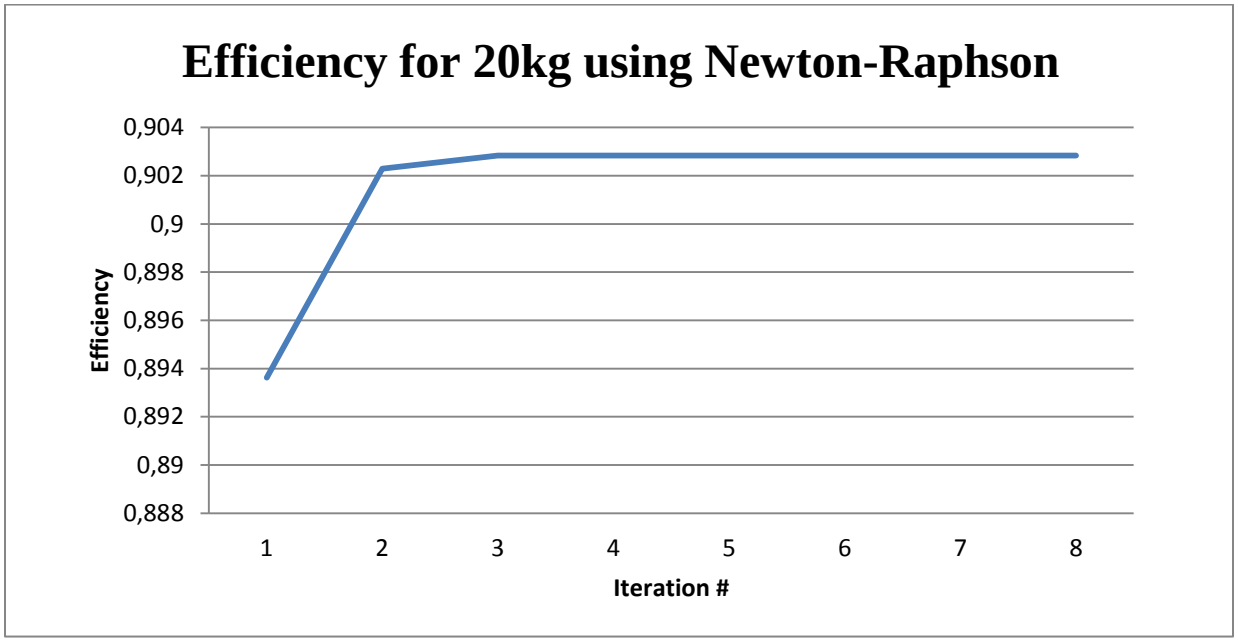

Figure 33 - Plot of efficiency vs. position during lowering for a 20kg-mass during Newton-Raphson

In obtaining the efficiency value for a 20kg mass, the figure obtained reveals that the range of values is from about 89.4% and converges at 90.35%. When compared to what was obtained for the 3-pulley travelling block system, we see a value slightly less than 88.15% as a starting point, then a convergent value slightly greater than 88.4%.

Clearly, this has followed the trend so far as to the fact that, the efficiency obtained for a 2-pulley travelling block system during hoisting is greater in value that for a 3-pulley travelling block system.

5.4.2.2.2 Efficiency for 20kg during lowering

The Newton-Raphson method when plotted on a graph produced the figure below. With reference to the figure, the efficiency value of the 20kg mass during lowering for a two-pulley travelling block system starts from about 65% and converges at 80%. This value obtained is in sharp contrast with what was obtained for a 3-pulley travelling block system where efficiency value begins from about 94.4% and converges at 98.4%.

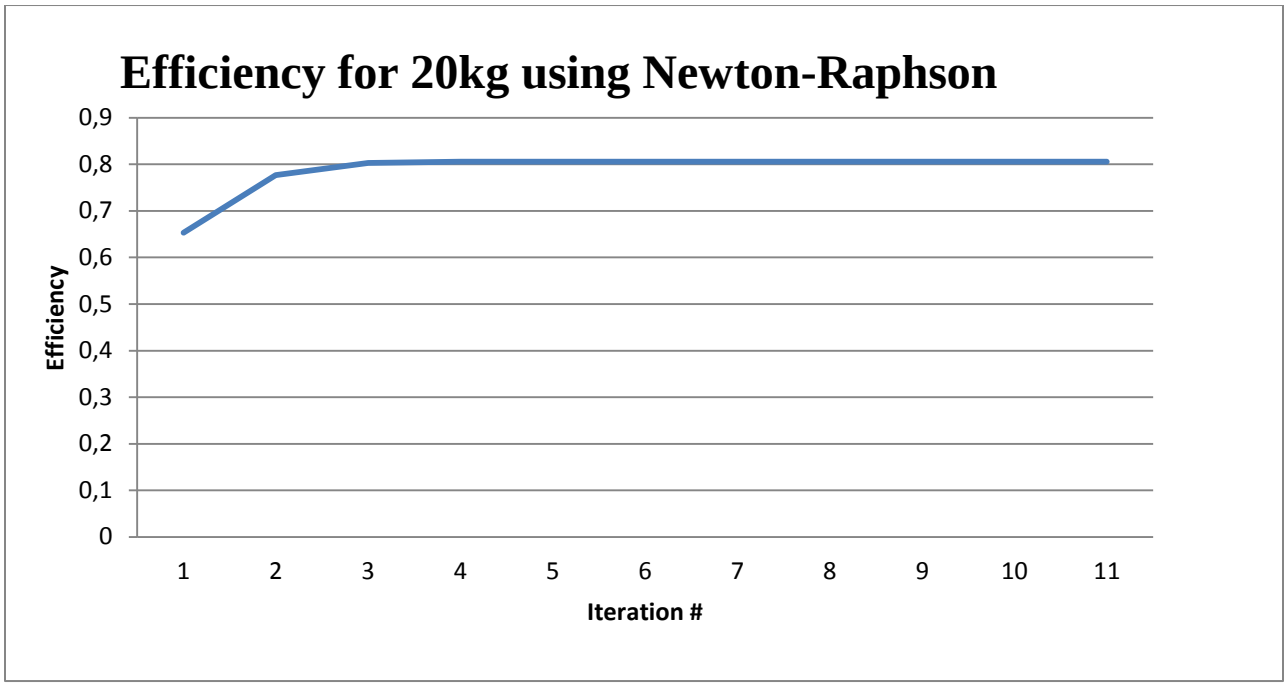

Figure 34 - Plot efficiency vs. position during lowering for a 20kg-mass using Newton-Raphson

Thus, the efficiency value for the two-pulley travelling block system is less than that obtained for a three-pulley travelling block system. This, again, is in agreement with what has been obtained so far for the 5kg.

5.4.2.2.3 Analysis for 20kg during hoisting

During hoisting for a 20kg, the above figure was obtained where before the weight is lifted off the ground, the hook load recorded is 0kg. As the weight is just lifted, the lines become taut which sharply increase the hook load reading at the dead line sensor from 0kg to about 4.5kg. in the course of the hoisting process, this value is fairly constant until the hoisting process is brought to an abrupt end.

This abrupt end marks a gentle increase in the value from 4.5kg to 5kg.

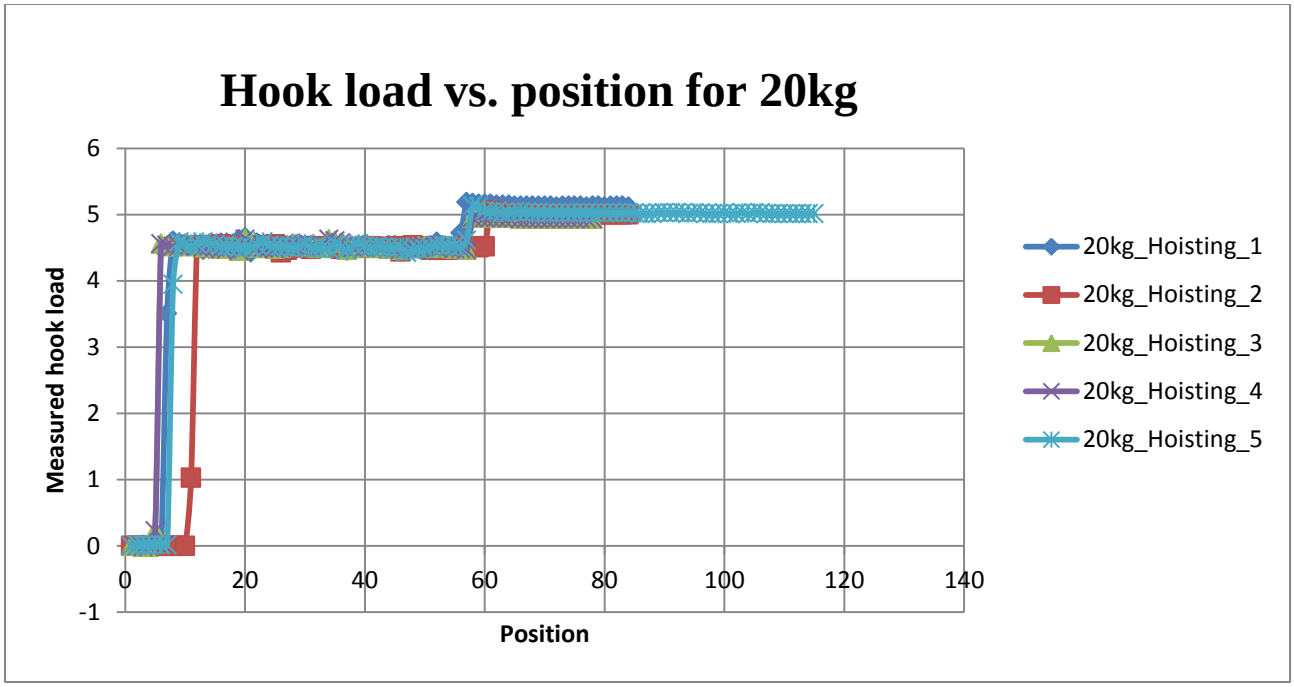

Figure 35 - Plot of hook load against position for five different experiments for 20kg

5.4.2.2.4 Analysis for 20kg during lowering

From a close look at the graph obtained above, four of the five experiments began from 5kg. That is, the previous hoisting history. However, one of the five starts from a value slightly above 4kg. This could be largely due to an error in the course of the experiment. Aside of that, as expected, the other four experimental readings began just where they were supposed to.

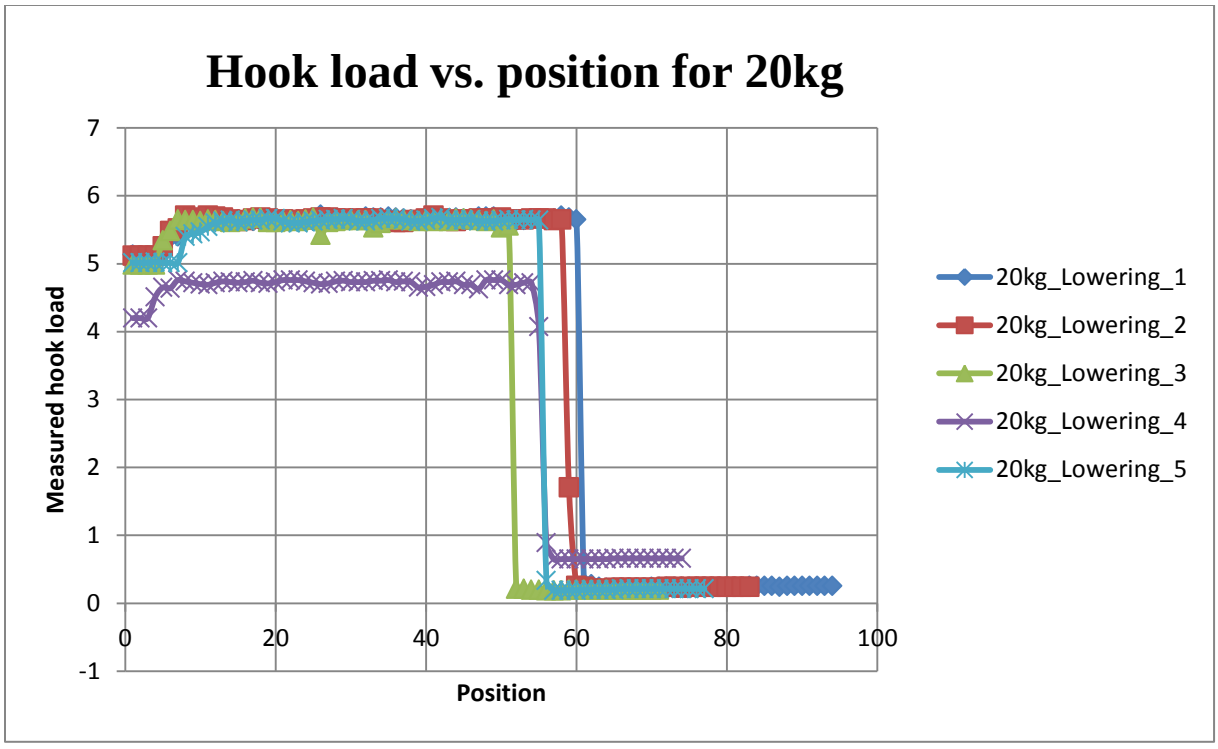

Figure 36 - Plot of hook load against position for five different experiments for 20kg

5.4.2.3 30kg weight

For the sake of consistency throughout this experiment, there was the need to have analysed the 40kg weight but not the 30kg. However, for a two-pulley system at the travelling block, only three pulleys are required at the crown block. The system was thus designed that each pulley in the crown block would accommodate a maximum weight of 10kg. Thus for a 3-pulley crown block arrangement, it only became necessary to limit the weight to a maximum total of 30kg, which couldn't be exceeded. This will in no way mar the effective analysis of the work. This is because the trend will still be observed as they already have been, irrespective of the individual weight.

5.4.2.3.1 Efficiency for 30kg hoisting

The plot for efficiency for the 30kg mass using the Newton-Raphson is as shown in the graph.

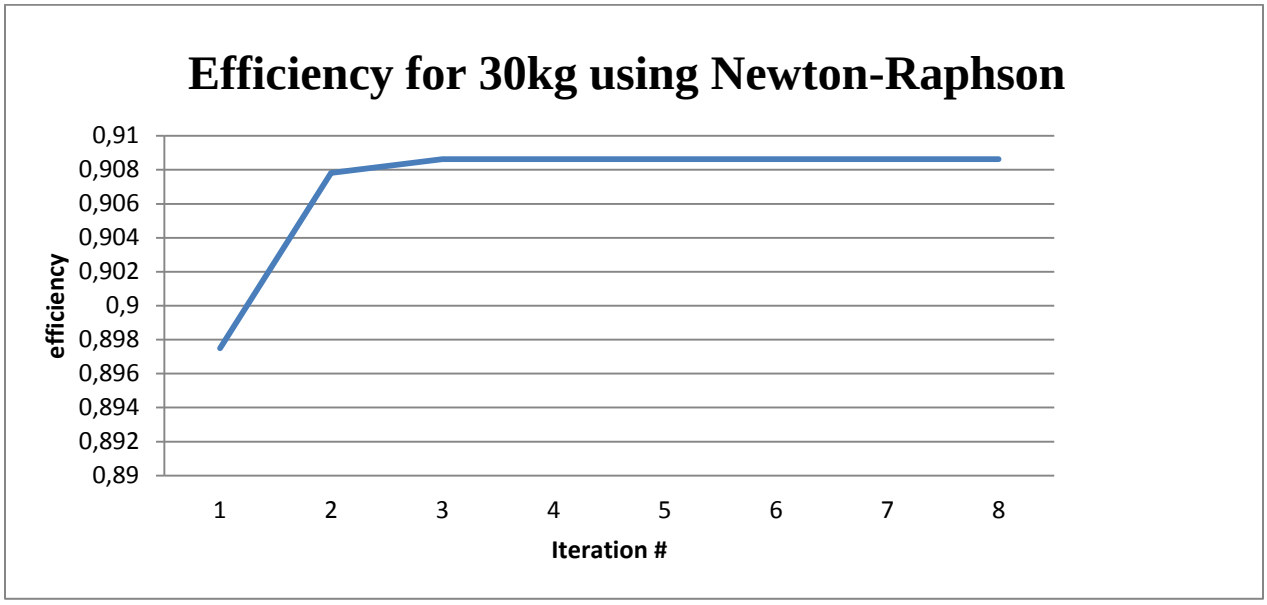

Figure 37 - Plot of efficiency vs. position during lowering for a 30kg-mass using Newton-Raphson

5.4.2.3.2 Analysis for 30kg during hoisting

Figure 38 shows the plot of hook load vs. position during the hoisting of a 30kg-mass

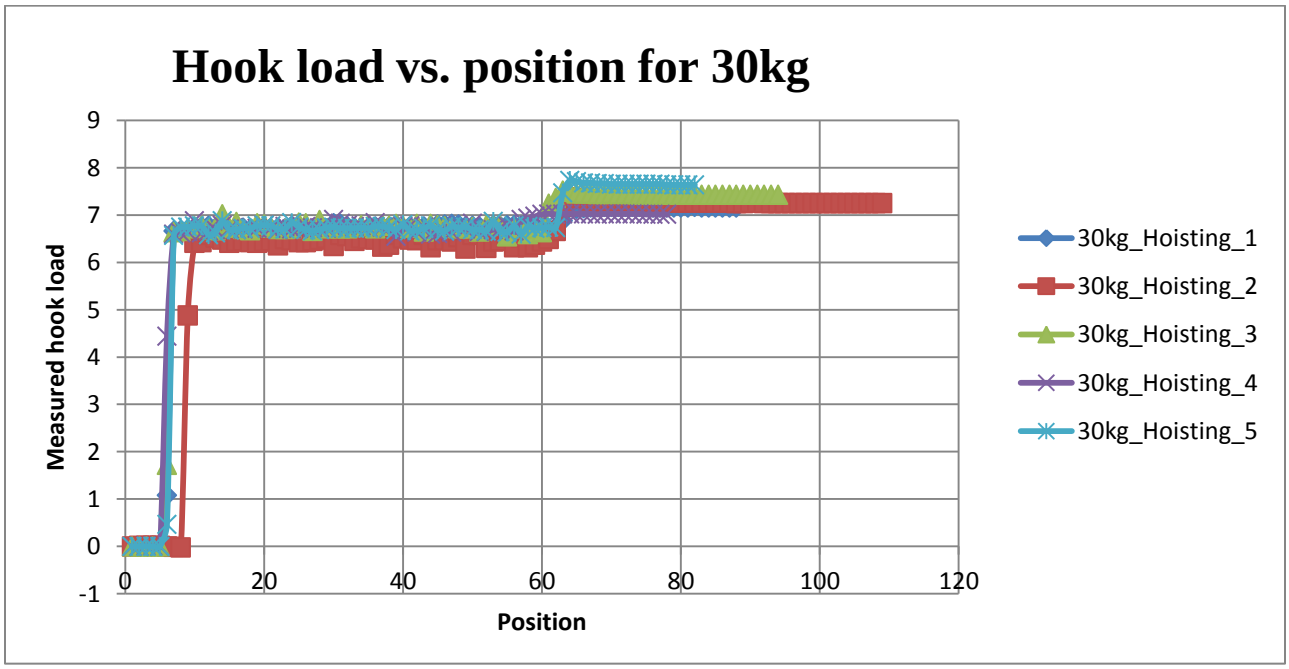

Figure 38 - Plot of hook load against position for five different experiments for 30kg

5.4.2.3.3 Efficiency for 30kg during lowering

Here, the figure shows the plot of efficiency using the iteration method of Newton-Raphson

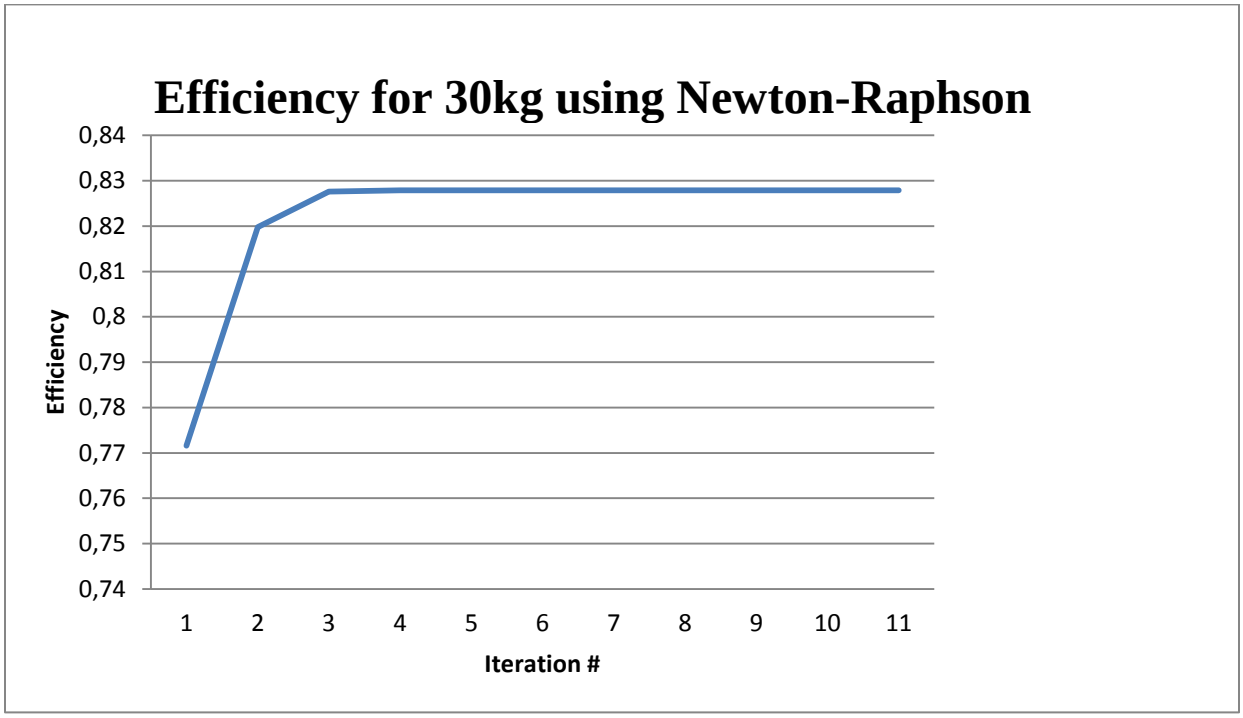

Figure 39 - Plot of efficiency vs. position during lowering for a 30kg-mass using Newton-Raphson method (lowering)

Starting from a value of 77.1% and convergent value of 82.9%, this represents the Newton-Raphson approach to calculating the efficiency for a 30kg mass during lowering with a 2-pulley travelling block system.

5.4.2.3.4 Analysis of 30kg during lowering

Figure 40 below indicates the plot of hook load vs. position during the lowering of a 30kg-mass.

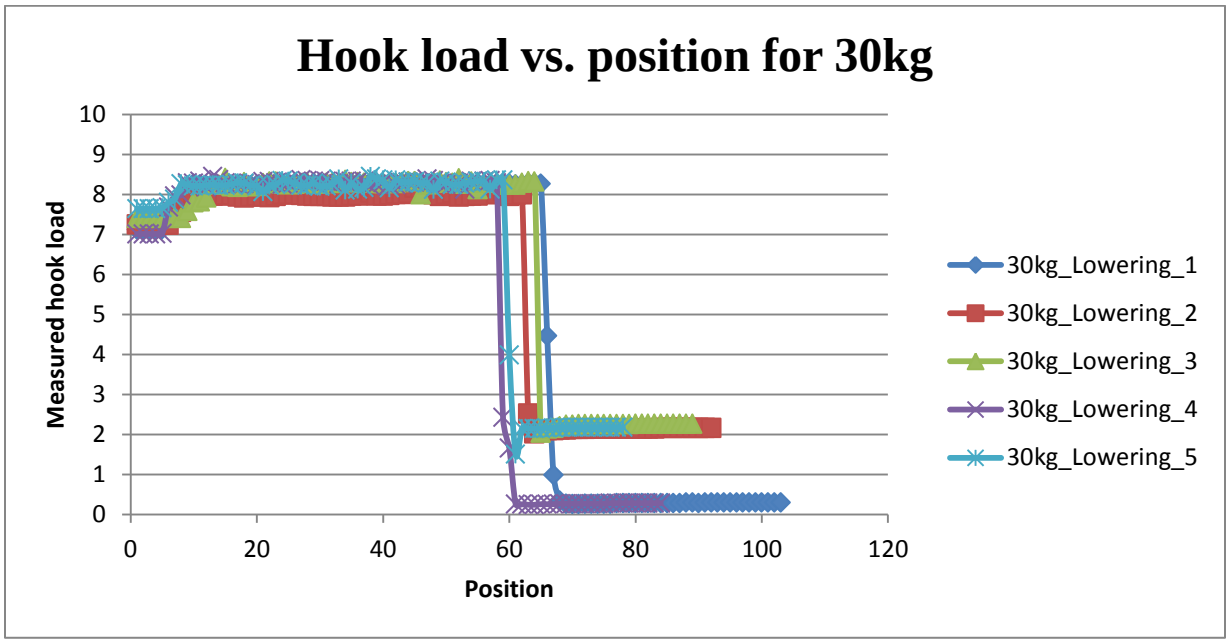

Figure 40 - Plot of hook load against position for five different experiments for 30kg

5.4.3 Four Lines

Here, the various efficiencies will be presented in a table.

Table 3: Efficiency of various weights for hoisting and lowering

Weight (kg)	Efficiency value recorded (%)	
	Hoisting	Lowering
5	88.16	99.6
20	91.78	99.99
40	95.5	99.99

5.4.4 Effect of linear weight of drill line

In developing the model, the effect of the drill line was investigated to ascertain its level of impact on the overall hook load reading.

With regards to the model equation developed, it was observed that the equation, $T_3 = F_{dl} + (L - l)g\bar{\lambda}_m$ governs the behaviour of the effect of the drill line on the hook load.

To be able to numerically and experimentally determine this, a program was written Excel where F_{dl}, that is, the reading at the dead line sensor, was made the subject of the relation.

In the above equation, it should be noted that L is the distance between the sensor on the dead-line and the closest block; which is also the inactive sheave. Fundamentally, one expects that L will be constant throughout the experiment. As such, any analysis would keep L as a constant.

Furthermore, l is the distance between the traveling and crown blocks. Depending on the movement of the traveling block, whether hoisting or lowering, the magnitude of l differed. This difference will be duly accounted for in the analysis to follow.

$\bar{\lambda}_m$ is also the mass per unit length of the drill line that is used. For different drill lines used, $\bar{\lambda}_m$ will differ, too. Then, g is the acceleration due to gravity. The acceleration due to gravity would have changes in sign, where positive (+) or negative (-) depending on the direction of movement of the travelling block. If hoisting, which is against gravity, then g assumes a negative (-) sign. When lowering, which is in favour of gravity, then g assumes a positive (+) sign.

5.4.4.1 Analysis with Excel program

5.4.4.1.1 Hoisting

When hoisting, l, which is the distance between the traveling and crown blocks, will decrease in magnitude. Also, g, the acceleration due to gravity will assume a negative (-) sign. From this understanding, the governing equation becomes $F_{dl} = T + Lg\bar{\lambda}_m - lg\bar{\lambda}_m$. Since the tension, T, could be considered constant at any position, and the expression, $Lg\bar{\lambda}_m$, is constant for a given mass per unit length of a drill line and a fixed distance between the dead line sensor and the inactive sheave, F_{dl}, which is the reading at the dead line sensor is dependent on $-lg\bar{\lambda}_m$.

From the simple Excel program that was used in the analysis, the following graph was as a result.

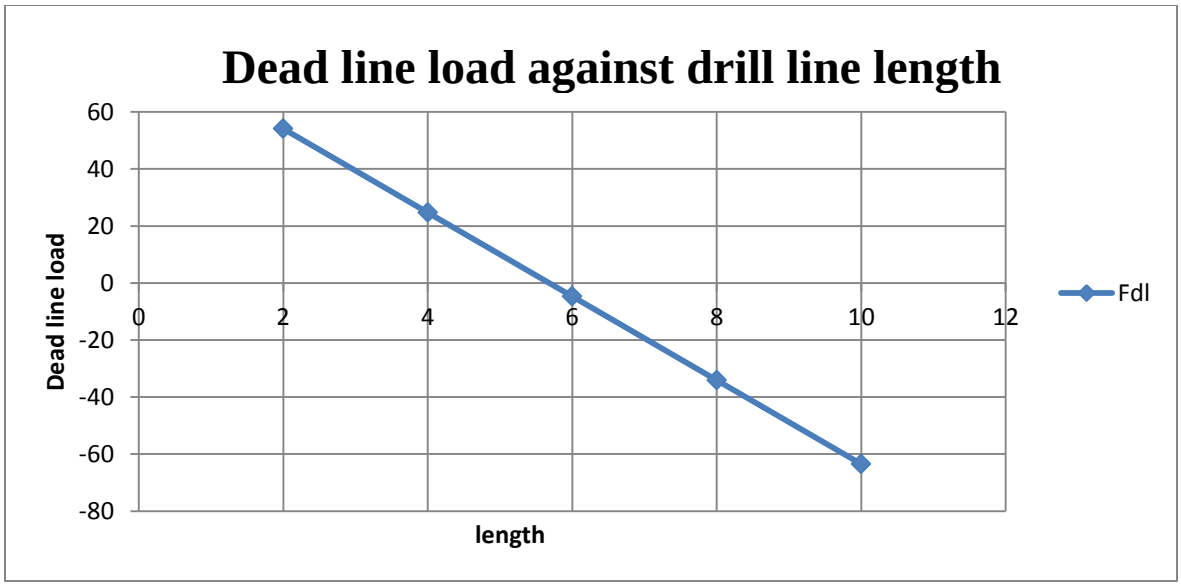

Figure 41 - Graph of Fdl against l

From the graph, it is evident that there is a negative relationship between F_{dl} and l. So that, during the process of hoisting, l decreases in magnitude. Thus for higher numerical magnitudes of l, smaller magnitudes of F_{dl} are observed.

This thus confirms that during hoisting, when the travelling block travels from the floor to the crown block where l is very minimal, F_{dl} assumes minimal values, too.

5.4.5.1.2 Lowering

The process of lowering is largely the reverse of hoisting. In that, during lowering of the travelling block from close to the crown block to the floor, the distance between the travelling block, l increases. Also, since lowering is in favor or the acceleration due to gravity, g assumes a positive (+) values.

Thus the governing equation for lowering becomes $F_{dl} = T - Lg\bar{\lambda}_m + lg\bar{\lambda}_m$. Keeping the tension, T, and expression, $Lg\bar{\lambda}_m$, constant, the F_{dl} now has a positive relationship with $lg\bar{\lambda}_m$. Hence for greater l values, which is what is observed during lowering, we will observer increasing values of F_{dl}.

The graph below depicts the observation;

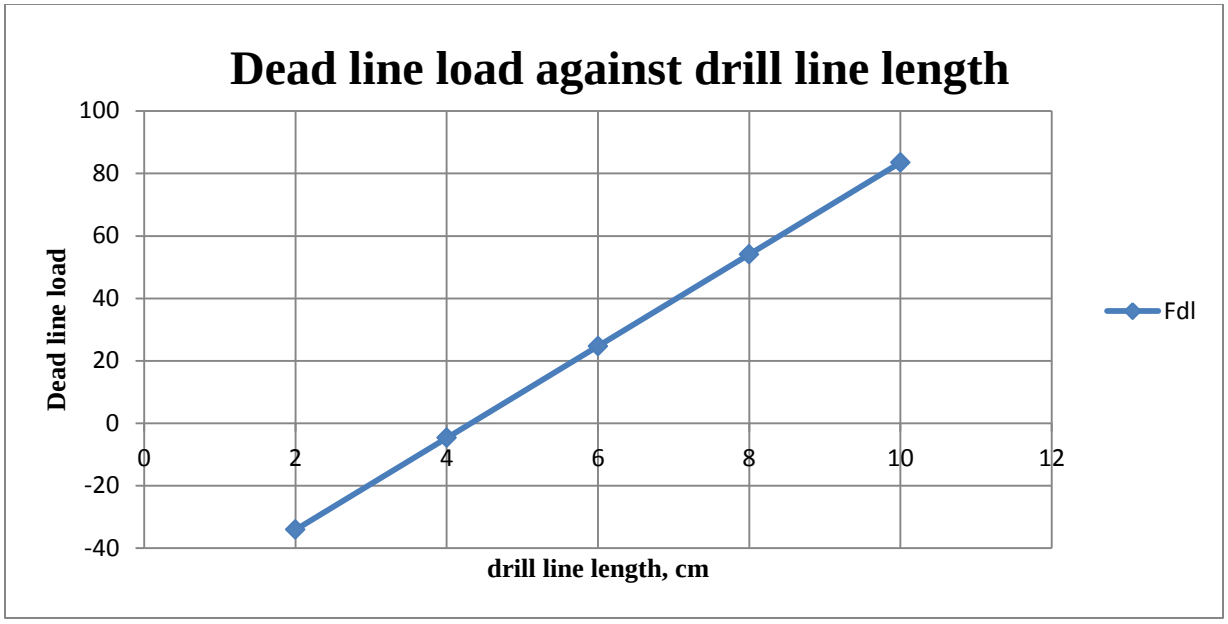

Figure 42 - Graph of Fdl against l

5.4.5.1.3 Effect of weight per unit length of drill line

From our governing equations, that is, $F_{dl} = T + Lg\bar{\lambda}_m - lg\bar{\lambda}_m$ for hoisting, and $F_{dl} = T - Lg\bar{\lambda}_m + lg\bar{\lambda}_m$ for lowering, it implies that at the same position, that is a constant value of l for both hoisting and lowering, changes in $\bar{\lambda}_m$, the weight per unit length of the drill line influences F_{dl}. And this is essentially what we aim to analyse in this section.

To do this, different weights per unit length of different drill lines were used and their impact on the value of F_{dl} were recorded and presented in the table below;

Table 4: Readings at the dead line sensor given varied drill lines with different weights per unit length during hoisting

Hoisting	
$\bar{\lambda}_m$(kg/m)	**F_{dl}(kg)**
0.5	-14.5
1.0	-39
1.5	-63.5
2.0	-88
2.5	-112.5

Table 5: Readings at the dead line sensor given varied drill lines with different weights per unit length during lowering

Lowering	
$\bar{\lambda}_m$(kg/m)	**F_{dl}(kg)**
0.5	34.5
1.0	59.0
1.5	83.5
2.0	108
2.5	132.5

It should be noted that each reading was analysed at a constant position, l. This was to ensure that the full effect of the weight per unit length of the drill line, $\bar{\lambda}_m$ was fully felt on the dead line sensor reading F_{dl}.

These tables of values were then plotted and the following graphs obtained;

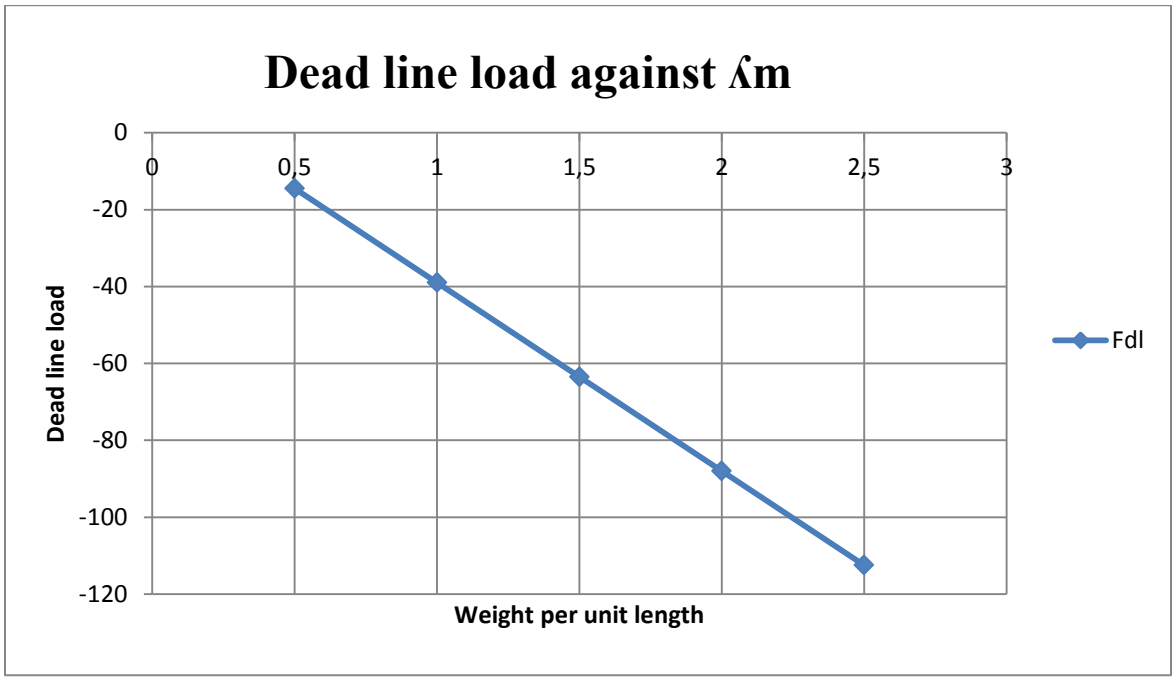

Figure 43 - Graph of Fdl against weight per unit length during hoisting

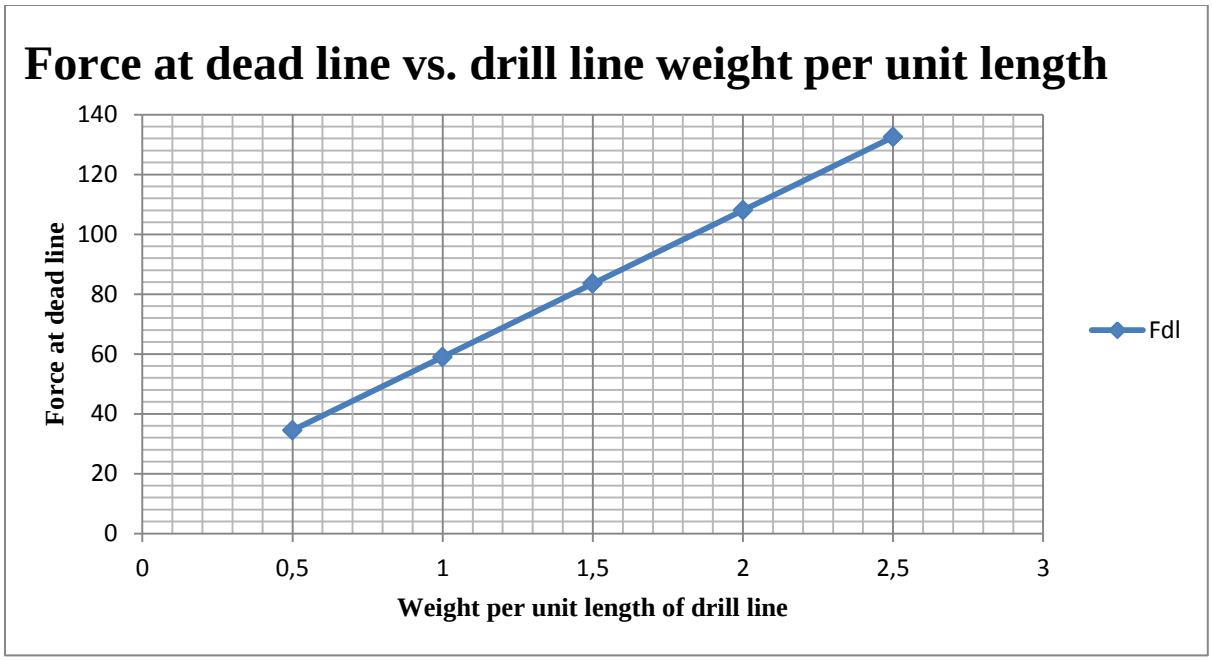

Figure 44 - Graph of Fdl against weight per unit length during lowering

The above graphs therefore imply that for increasing values of the weight per unit length of the drill line, negatively increasing values of the dead line sensor reading will be recorded during hoisting, while positively increasing values of the dead line sensor reading will be recorded during lowering. We thus investigate some more with our experimental values obtained from our rig setup.

5.4.5.2 Analysis with experimental data

In order to investigate the effect of the weight per unit length of a drill line on the dead line tension, two different lines with different weight per unit length were used in turns for the same weights and readings recorded.

5.4.5.2.1 Hoisting and weight per unit length

5kg weight

Table 6: Hook load readings for two different drill lines for a weight of 5kg for hoisting

As can be seen from the table, hook load values are obtained for the two different drill lines with ʎm = 0.0171kg/m and 0.03036kg/m at the same position.

No.	Hook load_average	Hook load with wire	Difference	% change
6	0,0026666	0,0293326	0,026666	90,90909
7	0,1493296	0,0613318	-0,0879978	-143,478
8	0,5359866	0,1493296	-0,386657	-258,929
9	0,8106464	0,3279918	-0,4826546	-147,154
10	0,8053132	0,5653192	-0,239994	-42,4528
84	0,8053132	0,7093156	-0,0959976	-13,5338
85	0,8319792	0,7093156	-0,1226636	-17,2932
86	0,8559786	0,7093156	-0,146663	-20,6767
87	0,866645	0,7093156	-0,1573294	-22,1805
88	0,8746448	0,7093156	-0,1653292	-23,3083
				-76,5563

To be able to determine the changes in the dead line sensor reading due to differences in the weight per unit length of each drill line, the difference between the hook loads is determined and the percentage change calculated. An average value of the percentage change in the hook load is also calculated to have a general overview of the impact of the differences in the different weight per unit length values.

From the table, it can be deduced that less hook load readings are obtained for the heavier drill line with ʎm = 0.0171kg/m. This observation tallies with what was determined in our simple Excel program.

To better conclude on our findings, the following tables also show what we observed for 20kg during hoisting;

Table 7: Hook load readings for two different drill lines for a weight of 20kg during hoisting

From the table above, a similar observation is made with an average percentage change in the recorded hook load as -30.6083%.

Position	Hook load with wire	Hook load	Difference	% change
7	0,0613318	0,4613218	-0,39999	-86,7052
8	0,239994	1,4292976	-1,1893036	-83,209
9	0,7946468	1,9652842	-1,1706374	-59,5658
10	1,3093006	2,586602	-1,2773014	-49,3814
84	2,6426006	2,6026016	0,039999	1,536885
85	2,6426006	2,6106014	0,0319992	1,225741
86	2,6426006	2,613268	0,0293326	1,122449
87	2,6452672	2,6372674	0,0079998	0,303337
88	2,639934	2,6612668	-0,0213328	-0,8016
				-30,6083

However, certain pockets of positive values were recorded. These are undoubtedly due to some experimental error. They however do not mar the ultimate experimental value and observation in any way.

5.4.5.2.2. Lowering and weight per unit length of drill line

In a similar vein, tables of lowering of various weights at the traveling block were recorded.

5kg weight

Table 8: Hook load readings for two different drill lines for 5kg during lowering

Position	Hook load with wire	Hook load_average	Difference	% change
6	1,0239744	1,2346358	-0,2106614	-20,5729
7	1,2853012	1,2639684	0,0213328	1,659751
8	1,3386332	1,2773014	0,0613318	4,581673
9	1,3839654	1,3039674	0,079998	5,780347
10	1,413298	1,3146338	0,0986642	6,981132
84	0,826646	0,1786622	0,6479838	78,3871
85	0,6613168	0,1786622	0,4826546	72,98387
86	0,831090333	0,1786622	0,652428133	78,50267
87	0,759981	0,1813288	0,5786522	76,14035
88	0,759981	0,1813288	0,5786522	76,14035
				38,05843

During the process of lowering, it can be observed that higher values were obtained for the drill line with higher weight per unit length. This also further confirms the initial observation made with the Excel program.

20kg weight

Table 9: Hook load readings for two different drill lines for 20kg during lowering

An overall percentage increase of about 28.64 is recorded following the use of the drill line with a weight per unit length of 0.03036kg/m than that of 0.0171kg/m.

Position	Hook load with wire	Hook load	Difference	% change
6	3,9012358	3,7119072	0,1893286	4,853042
7	3,9012358	3,7492396	0,1519962	3,896104
8	3,9945668	3,786572	0,2079948	5,206943
9	4,0238994	3,8052382	0,2186612	5,434062
10	4,0425656	3,8159046	0,226661	5,60686
84	0,5439864	0,2026616	0,3413248	62,7451
85	0,5439864	0,2026616	0,3413248	62,7451
86	0,3706574	0,2026616	0,1679958	45,32374
87	0,3706574	0,2026616	0,1679958	45,32374
88	0,3706574	0,2026616	0,1679958	45,32374
				28,64584

From the Excel program and experiment, it can be concluded thus that a higher weight per unit length of a drill line has a negative (in terms of magnitude) impact on the dead line sensor reading; while a higher weight per unit length has a positive (also, in terms of magnitude) impact on the dead line sensor reading.

5.4.5 Effect of dolly retraction

The process of retracting the dolly becomes essential while making a connection. During this process, the center of the well is readily available to add more pipes. For the addition of pipes to be realized, the travelling block equipment is pulled away from the center of the well to make for space. The process of pulling the travelling block equipment from the center of the well is therefore achieved by retracting the dolly and connected to the travelling block.

During the experiment, a similar process was simulated to observe and analyse what effect this process of retraction of the dolly and its connection to the travelling block has on the resultant hook load in the process.

This analysis will therefore be done comparing hook load data during our dolly retraction, with during a normal process of hoisting and/or lowering.

5.4.5.1 Analysis from the model

From the model, the diagram below was used in the derivation of the resulting force on the travelling block due to the process of dolly retraction.

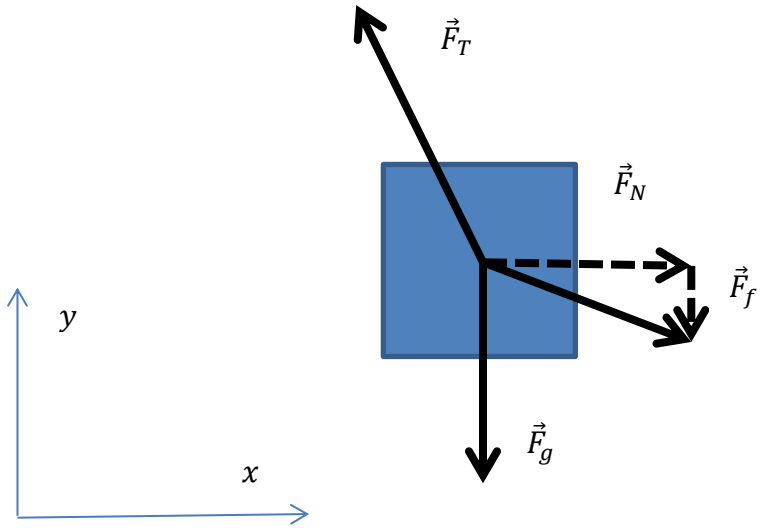

When the travelling block is retracted, the drill lines which were initially vertical make an angle θ with the vertical. As was shown in chapter four, the resulting force on the travelling block becomes $F_T = \frac{mg}{(\cos\theta + sign(v)\mu_d \sin\theta)}$. When we take a closer look at the denominator of the expression, it will be observed that since θ is an angle less than 90 degrees, and μ_d, is a friction co-efficient with typical values less than 1, it implies the denominator will be less than 1, which means the total value of F_T is greater in magnitude that during an ordinary operation without dolly retraction. This will be further observed in the experimental data reporting.

5.4.5.2 Experimental data reporting for dolly retraction

In this section, we analyse the data values for two different weights; 20kg and 40kg.

20kg weight hoisting

Table 10: Comparison of hook load readings for dolly retraction and normal operation for 20kg during hoisting

No.	Hook load_dolly retraction	Hook load	Difference	% change
6	0,0053332	0,0053332	0	0
7	0,746648	0,4613218	0,2853262	38,21429
8	1,453297	1,4292976	0,0239994	1,651376
9	2,1172804	1,9652842	0,1519962	7,178841
10	2,2852762	2,586602	-0,3013258	-13,1855
84	2,8692616	2,6026016	0,26666	9,29368
85	2,8719282	2,6106014	0,2613268	9,09935
86	2,8612618	2,613268	0,2479938	8,667288
87	2,8505954	2,6372674	0,213328	7,48363
88	2,8372624	2,6612668	0,1759956	6,203008
				7,460593

The second column indicated, “Hook load_dolly retraction” is the set of average data recorded when the dolly was retracted with the travelling block which contained the 20kg weight was hoisted. For the same weight, the travelling block is left in normal mode without any form of retraction. Average values were also recorded and indicated as “hook load”.

To be able to ascertain the effect of the dolly retraction on the overall hook load reading, the “hook load” readings are subtracted from the “hook load_dolly retraction” and the difference recorded as indicated in the fourth column as “differences”. Percentage-wise, we then calculate the percentage increase in the hook load following the dolly retraction, taking the “hook load_dolly retraction” as the basis of comparison.

As indicated in the column labelled, “% change”, we can observe that the hook load due to dolly retraction is quite more in magnitude as compared to the hook load recorded during normal operation (that is, no dolly retraction). As an average, it shows that the readings of the “hook load_dolly retraction” are generally about 7.46% higher in magnitude than that of “hook load”

20kg lowering

Table 11: Comparison of hook load readings for dolly retraction and normal operation for 20kg during lowering

No.	Hook load_dolly retraction	Hook load	Difference	% changing
6	3,6985742	3,7119072	-0,013333	-0,36049
7	4,0025666	3,7492396	0,253327	6,329114
8	4,026566	3,786572	0,239994	5,960265
9	4,0372324	3,8052382	0,2319942	5,746367
10	4,053232	3,8159046	0,2373274	5,855263
84	0,2346608	0,2026616	0,0319992	13,63636
85	0,2319942	0,2026616	0,0293326	12,64368
86	0,226661	0,2026616	0,0239994	10,58824
87	0,2239944	0,2026616	0,0213328	9,52381
88	0,2239944	0,2026616	0,0213328	9,52381
				7,944642

In the drilling process when the dolly is retraction and connected to the travelling block and hoisted into the crown block for more pipes to be added, it is lowered along the dolly rails and a re-connection made for drilling to commence again. During this process of lowering, the sensor at the dead line continues to take readings of the hook load that results in the drill lines.

From the table presented, it's clear that the process of lowering during dolly retraction results in a higher hook load reading than when it's in normal operation. It indicates that the readings made during dolly retraction in a lowering mode are about 7.94% higher on average than during a normal operation without dolly retraction.

40kg weight hoisting

Table 12: Comparison of hook load readings for dolly retraction and normal operation for 40kg during hoisting

In a similar vein as that of the 20kg weight, the hook load readings for 40kg as is indicated in the figure below during hoisting and dolly retraction is higher in magnitude than that during a normal process of hoisting without dolly retraction.

No.	Hook load (dolly retraction)	Hook load	Difference	% change
6	1,239969	0,0053332	1,2346358	99,56989
7	4,5758856	0,6346508	3,9412348	86,13054
8	5,5118622	2,5946018	2,9172604	52,92695
9	5,519862	4,679883	0,839979	15,21739
10	5,5225286	5,266535	0,2559936	4,635442
84	5,5625276	5,573194	-0,0106664	-0,19175
85	5,5838604	5,5411948	0,0426656	0,764088
86	5,6425256	5,6025266	0,039999	0,708885
87	5,6318592	5,6105264	0,0213328	0,378788
88	5,7491896	5,6211928	0,1279968	2,226345
				26,23666

An average value of about 26.24% on average is recorded as higher than of a normal hoisting process. Beyond that, it is worthy to note that this value of 26.24% is, of course, larger than what was obtained with the 20kg weight during hoisting in a dolly retraction mode. An average value of 7.46% was obtained for the 20kg.

This also confirms the model where $F_T = \frac{mg}{(\cos\theta + sign(v)\mu_d \sin\theta)}$. From the relation, F_T, is directly proportional to mg. Therefore, it is expected that the higher the weight on the travelling block equipment, the higher the resulting value for F_T which would thus translate into a higher value for the hook load.

40kg lowering

The process of lowering with a mass of 40kg also produces similar results with the hook load due to dolly retraction being about 41.97% higher on average than of a normal process.

No.	Hook load_dolly retraction	Hook load	Difference	% change
6	7,4104814	3,7119072	3,6985742	49,91004
7	7,5491446	3,7492396	3,799905	50,33557
8	7,5491446	3,786572	3,7625726	49,84105
9	7,5891436	3,8052382	3,7839054	49,85945
10	7,5918102	3,8159046	3,7759056	49,73656
84	0,2959926	0,2026616	0,093331	31,53153
85	0,3039924	0,2026616	0,1013308	33,33333
86	0,3093256	0,2026616	0,106664	34,48276
87	0,3119922	0,2026616	0,1093306	35,04274
88	0,3146588	0,2026616	0,1119972	35,59322
				41,96663

Another interesting trend worthy of observation is that the hook load values recorded for the both weights are higher in the process of lowering than hoisting. Though this observation is less pronounced in the 20kg, where an increase in hook load of 7.46% and 7.94% were recorded for hoisting and lowering respectively, an increase in hook load of 26.24% and 41.97% were also recorded for hoisting and lowering respectively in the case of the 40kg weight.

5.4.6 Effect of mud hose and top-drive umbilical

To be able to rightly simulate the effects of the mud hose and top-drive umbilical on the resultant hook load that is registered at the dead line sensor, a chain was hanged from the frame of the experimental rig and hanged unto the travelling block equipment.

Rounds of hoisting and lowering were carried out with various weights, while the hook load results are recorded. These will be analysed in this section for a full understanding of how they could also impact the hook load readings.

5kg hoisting

Table 13: Comparison of hook load with chain and normal operation for 5kg hoisting

From the table below, each hook load reading for when there is chain and no chain are measured at the same positions to ensure accuracy in comparison and analysis. It can be observed from the table that the second column with "Hook load with chain" has values of greater magnitude than those of "hook load" at the same position.

Position	Hook load with chain	Hook load	Difference	% change
6	0,1519962	0,0026666	0,1493296	98,24561
7	0,7253152	0,1493296	0,5759856	79,41176
8	1,0293076	0,5359866	0,493321	47,92746
9	0,9786422	0,8106464	0,1679958	17,16621
10	0,946643	0,8053132	0,1413298	14,92958
84	0,9653092	0,8053132	0,159996	16,57459
85	0,9679758	0,8319792	0,1359966	14,04959
86	0,9679758	0,8559786	0,1119972	11,57025
87	0,9653092	0,866645	0,0986642	10,22099
88	0,9679758	0,8746448	0,093331	9,641873
				31,97379

Thus differences are found between each hook load value and recorded under the section with "Difference". The percentage change due to the chain is then calculated and recorded under the section with "% change". Since all the values under "% change" are positive, it implies that at every stage of the hoisting operation, the connection of the chain on the travelling block exerts a certain vertical tension, $T_v$which is aptly captured in the model equation as $T_v(x) = \frac{g\partial_s m_{mh}}{2a}\sinh\frac{x}{a}$

Due to this extra vertical tension as a result of the connection of the chain, in the case of our experiment, we expect for the resultant hook load to be greater in magnitude than in the case without a chain connected.

20kg hoisting

Table 14: Comparison of hook load with chain and normal operation for 5kg hoisting

Position	Hook load_chain	Hook load	Difference	% change
6	0,0079992	0,0053332	0,002666	49,98875
7	0,3439782	0,4613218	-0,1173436	-25,4364
8	2,7598014	1,4292976	1,3305038	93,08795
9	2,826467	1,9652842	0,8611828	43,81976
10	2,8024688	2,586602	0,2158668	8,345575
84	2,837134	2,6026016	0,2345324	9,01146
85	2,8344674	2,6106014	0,223866	8,575265
86	2,8398	2,613268	0,226532	8,668533
87	2,8318008	2,6372674	0,1945334	7,376324
88	2,8184702	2,6612668	0,1572034	5,907089
				20,93443

A similar observation was also made with the hoisting of the 20kg weight plus the chain. However, an anomaly is observed with the result at the 7th position where it's apparent that the hook load reading for a normal operation (without chain connected) is greater than with a chain connected. This, undoubtedly, is most likely due to some error in the experimental procedure. Aside of that, all other values are as expected. As an average, it can be seen that the hook load readings made with chain connected is about 20.93% higher than those without a chain.

5kg lowering

Table 15: Comparison of hook load with chain and normal operation for 5kg lowering

No.	Hook load_chain	Hook load_average	Difference	% change
6	1,4292976	0,0026666	1,426631	53500
7	1,4612968	0,1493296	1,3119672	878,5714
8	1,479963	0,5359866	0,9439764	176,1194
9	1,4959626	0,8106464	0,6853162	84,53947
10	1,5012958	0,8053132	0,6959826	86,42384
84	0,66665	0,8053132	-0,1386632	-17,2185
85	0,4586552	0,8319792	-0,373324	-44,8718
86	0,3946568	0,8559786	-0,4613218	-53,8941
87	0,1893286	0,866645	-0,6773164	-78,1538
88	0,186662	0,8746448	-0,6879828	-78,6585

The data collected for the lowering for a 5kg weight is rather erroneous as it produced values far beyond our limit of expectation. This is testimony to the fact that the experiment that was performed was not perfect. However, the values so far show that the experimental values are highly dependable for a safe conclusion.

20kg lowering

Table 16: Comparison of hook load with chain and normal operation for 5kg hoisting

Position	Hook load with chain	Hook load	Difference	% change
6	3,853237	3,7119072	0,14133	3,807471
7	3,8719032	3,7492396	0,122664	3,271693
8	3,8959026	3,786572	0,109331	2,887324
9	3,9492346	3,8052382	0,143996	3,784163
10	3,9839004	3,8159046	0,167996	4,402516
84	0,213328	0,2026616	0,010666	5,263158
85	0,2079948	0,2026616	0,005333	2,631579
86	0,2053282	0,2026616	0,002667	1,315789
87	0,2053282	0,2026616	0,002667	1,315789
88	0,2079948	0,2026616	0,005333	2,631579
				3,131106

A more accurate observation is made with the lowering process of a 20kg weight. As an average, we record a percentage increase in hook load of about 3.13% when the chain is connected than when in normal operation (no chain connected).

6 Conclusion

The goal of this thesis work was to investigate the effect of factors such as the drill line weight per unit length, the dolly retraction and the mud hose and top-drive umbilical. This was to be achieved by the development of a mathematical model. This model will thus be analysed using experimental data obtained from a rig set up that was built purposefully for this thesis work.

From the experiments, it is obvious that the factors that were investigated have some effects on the hook load readings that are recorded by the dead line sensor. Generally, the following could be reported;

- Drill line: Lower hook load readings were recorded for drill line with a higher weight per unit length. On the contrary, higher hook loads were observed in the case of drill line with relatively less weight per unit length. In the same vein, drill line with relatively higher weight per unit length recorded negatively less hook load values during hoisting, while drill line with relatively less weight per unit length recorded positively higher hook load.

- Dolly retraction: It was also observed that during a change in pipe where it becomes necessary to pull the travelling block away from the well center, the process of retracting the dolly and attaching it to the travelling block, while hoisting or lowering has some effects on the hook load readings. This was made clear by the positive differences that were observed in the hook load during retraction and normal operation (no dolly retraction).

- The mud hose and top-drive umbilical also have a vertical tensional pull on the travelling block.

With these factors duly investigated and documented, it is clear that there is more work to do to improve on the currently-used model for calculating hook load in the oil and gas industry.

References

1. Stuck Pipe Book by Drilling Formulas (Page 5)
2. Wikipedia. 2014. Weight on Bit http://en.wikipedia.org/wiki/Weight_on_bit
3. http://www.facebook.com/l.php?u=http%3A%2F%2Fwww.google.no%2Furl%3Fsa%3Dt%26rct%3Dj%26q%3D%26esrc%3Ds%26source%3Dweb%26cd%3D8%26cad%3Drja%26ved%3D0CGUQFjAH%26url%3Dhttp%253A%252F%252Fintinno.iitkgp.ernet.in%252Fcourses%252F1192%252Fwfiles%252F237157%26ei%3DiakEU5rWG-jb4QTX4YDQBg%26usg%3DAFQjCNGBYAfk6C1AcAzaGVJdAPbKXoj0XA%26sig2%3DyjdRpaOpqi_v5yDJQvOFig%26bvm%3Dbv.61535280%2Cd.bGE&h=SAQEpStyj
4. Drilling Engineering – PE 311 by Tan Nguyen (page 4)
5. Calculating RPM (page 1)
6. Wikipedia. 2014. Rate of penetration http://en.wikipedia.org/wiki/Rate_of_penetration
7. Managing Drilling Risk by Walt Aldred, Dick Plumb (Sugar Land, Texas, USA); Ian Bradford, John Cook, Vidhya Gholkar (Cambridge, England); Liam Cousins, Reginald Minton, (BP Amoco Plc, Aberdeen, Scotland); John Fuller (Gatwick, England); Shuja Goraya (Cabinda, Angola); Dean Tucker (Aberdeen, Scotland).
8. Fundamentals of Drilling Engineering (SPE textbook series vol. 12) by Robert F. Mitchell, Stefan Z. Miska
9. Schlumberger oilfield glossary. 2014. Hook load http://www.glossary.oilfield.slb.com/en/Terms.aspx?LookIn=term%20name&filter=hook%20load
10. Johancsik, C.A., Friesen, D.B. and Dawson, R. 1984. Torque and Drag in Directional Wells – Prediction and Measurement. Journal of Petroleum Technology. June 1984.
11. Aadnoy, B.S., Fazaelizadeh, M. and Hareland, G. 2010. A 3D Analytical Model for Wellbore Friction. Journal of Canadian Petroleum Technology 49 (10): 25-36. SPE-141515-PA.
12. Wikipedia. 2014. Draw-works http://en.wikipedia.org/wiki/Draw-works

13. Schlumberger oilfield glossary. 2014. Draw-works http://www.glossary.oilfield.slb.com/en/Terms.aspx?LookIn=term%20name&filter=draw works
14. Petroleum Drilling Equipment by the China Aviation Oil Import and Export Corporation (page 4)
15. https://www.metu.edu.tr/~kok/pete110/PETE110_CHAPTER7.pdf page 55
16. http://petrofed.winwinhosting.net/upload/PRESENTATION%205.pdf page
17. http://pointapex.com/oilfield/XJ250S-drawworks.pdf
18. http://www.eng.cu.edu.eg/users/aelsayed/Hoisting.pdf
19. Determination of True Hook Load and Line Tension Under Dynamic Conditions by G.R. Luke, SPE, and H.C. Juvkam-Wold, SPE, Texas A&M U.
20. Estimation of Weight and Torque on Bit: Assessment of Uncertainties, Correction, and Calibration Methods by Eric Cayeux, and Hans Joakim Skadsem, IRIS.
21. Mirhaj, S.A., Fazaelizadeh, M., Kaarstad, E. and Aadnoy, B.S. 2010. New Aspects of Torque-and-Drag Modeling in Extended-Reach Wells. Paper SPE 135719 presented at the SPE Annual Technical Conference and Exhibition, Florence, Italy, 19-22 September.
22. Evaluation of Hook-load Measurements in Drilling Rig Hoisting Systems by Eric Cayeux (International Research Institute of Stavanger).
23. Mme, U., Skalle, P., Johansen, S.T. et al. 2012. Analysis and modeling of normal hook load response during tripping operations. Technical report, Norwegian University of Science and Technology (NTNU), Norway (unpublished).
24. A New Concept Drilling Hoisting Systems Rigs by Jan Artymiuk, University of Science and Technology, Krakow, Poland.
25. Maidla, E.E., Wojtanowicz, A.K.(1987,a).Field Method of Assessing Borehole Friction for Directional Well Casing., Society of Petroleum Engineers, SPE Middle East Oil Show, Manama, Bahrain, March 7-10, 15696.
26. Maidla, E.E., Wojtanowicz, A.K. (1987,b). Field Comparison of 2-D and 3-D Methods for the Borehole Friction Evaluation in Directional Wells., Society of Petroleum Engineers. 62nd SPE Annual Technical Conference, Dallas, Texas September 7-10, 16663.

27. Kristensen, Edvin, Model of Hook Load During Tripping Operation, Norwegian University of Science and Technology, Department of Petroleum Engineering and Applied Geophysics.
28. Schooley, M.C., Wick, C. and Burgess, T. 1987. Designing Well Paths To Reduce Drag and Torque. SPE Drilling Engineering 2 (4): 344-350. SPE-15463-PA

List of abbreviations

WOB – Weight On Bit

RPM – Revolution Per Minute

ROP – Rate Of Penetration

HKL – Hook Load

iBOP – Internal Blow Out Preventer

AC – Alternating Current

DC – Direct Current

HPU – Hydraulic Power Unit

MPH – Meters Per Hour

NPT – Non-Productive Time

MD – Measured Depth

List of symbols

B_i	Symbol denoting the block
dL	An infinitesimal pulley displacement [L]
dN	An infinitesimal normal force [MLT^{-2}](N)
ds	Length of a reference element of rope [L](m)
dT	An infinitesimal small tension variation [MLT^{-2}](N)
$d\theta$	An infinitesimal small angle [dimensionless](rd)
$\vec{F}_C$	Centrifugal force applied to the drill-line winded around the pulley [MLT^{-2}](N)
F_d	Force on the derrick [MLT^{-2}](N)
F_{dl}	Force on the dead-line [MLT^{-2}](N)
F_{dw}	Force on the draw-work line [MLT^{-2}](N)
$\vec{F}_L$	Total vector force applied by the pulley to its axle [MLT^{-2}](N)
$\vec{F}_R$	Reaction force between the axle and the pulley [MLT^{-2}](N)
$\vec{F}_W$	Weight of the pulley [MLT^{-2}](N)
F_{tb}	Force on the traveling blocks [MLT^{-2}](N)
g	Gravitational acceleration [LT^{-2}](m/s^2)
L	Distance between the sensor on the dead-line and the closest block [L](m)
l	Distance between the traveling and crown block [L](m)
$\vec{M}_f$	Frictional moment between the bearings and the pulley [ML^2T^{-2}](Nm)
m_p	Mass of the pulley [M](kg)
n	Number of lines supporting the traveling equipment
$\hat{r}$	Unit vector in the radial direction
r_a	Radius of the bearings of a pulley [L](m)
r_b	Radius of a pulley [L](m)
$\vec{T}_A$	Vector tension at contact point A [MLT^{-2}](N)
$\vec{T}_B$	Vector tension at contact point B [MLT^{-2}](N)
T_i	Tension in the drill-line [MLT^{-2}](N)

v Linear velocity of a short length of drill-line [LT^{-1}](m/s)

v_i Velocity of the drill-line at the level of the block i [MT^{-1}](m/s)

v_{tb} Velocity of the traveling block [MT^{-1}](m/s)

$\hat{y}$ Unit vector in the vertical direction

Greek letters:

ε Block efficiency [dimensionless](proportion)

$\bar{\lambda}_m$ Linear weight of the drill-line [ML^{-1}](kg/m)

θ Angle between the contact points of the drill-line with the pulley compared to the centre of rotation [dimensionless](rd)

ω Angular velocity [T^{-1}](rd/s)

μ_a Friction coefficient between the pulley and its axle [dimensionless]

μ_b Friction coefficient between the drill-line and the pulley [dimensionless]

List of figures

List of tables

Appendix

Derivation of the Luke and Juvkam Equations

Let us consider a draw-works based hoisting system with 2 traveling blocks, noted B_2 and B_4 and 3 crown-blocks, noted B_1 , B_3 and B_5 (see **Error! Reference source not found.**). Let us called the tensions at each extremities of the lines between anchoring points and pulleys T_i, starting from $i = 0$ at the deadline anchor and finishing at $i = 11$ at the draw-works spool. We will note $T_0 = F_{dl}$ and $T_{11} = F_{dw}$. We will note F_{tb} the force applied to the traveling blocks, and F_d the force applied to the derrick.

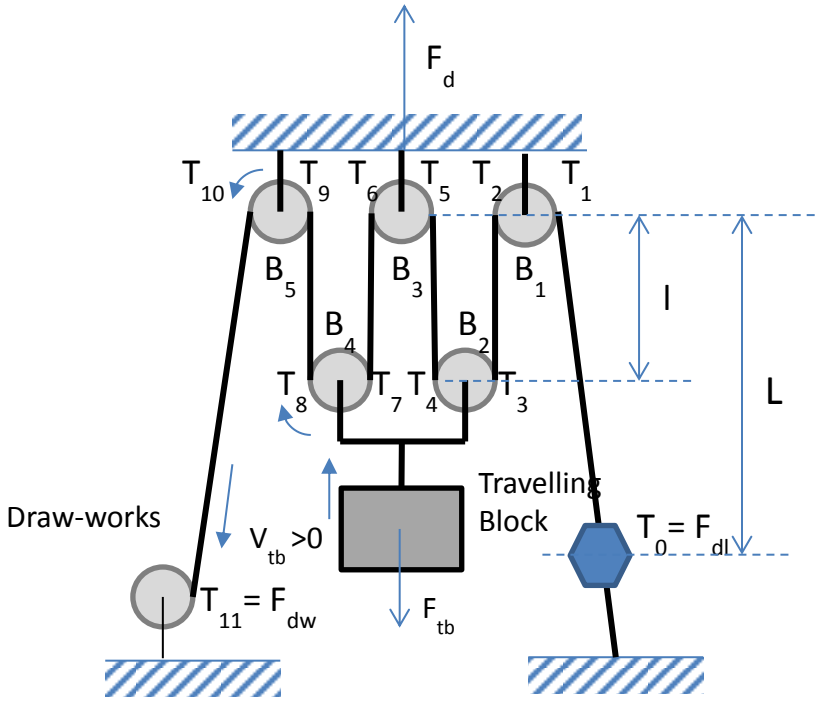

Schematic of a hoisting system based on a draw-works.

In the Luke and Juvkam model, the weight of the drill-line can be neglected and therefore the tensions are equal between the top and bottom of a line element in between two contact points ($T_0 = T_1, T_2 = T_3$, etc.).

We will first consider that since the block B_1 never rotates, there is no loss of tension on each of that pulley and therefore $T_2 = T_1 = F_{dl}$. At the level of each other pulleys, the pulley efficient shall be applied. Since friction always acts against the movement, when the traveling equipment is hoisted, $T_4 = \frac{T_3}{e}$, where e is the pulley efficiency. When the traveling block is lowered

$T_4 = eT_3$. By recursion, while raising, we obtain that $T_6 = \frac{T_5}{e} = \frac{F_{dl}}{e^2}$, $T_8 = \frac{T_7}{e} = \frac{F_{dl}}{e^3}$ and $T_{10} = \frac{T_9}{e} = \frac{F_{dl}}{e^4}$. Similarly, when lowering, we have $T_6 = eT_5 = e^2F_{dl}$, $T_8 = eT_7 = e^3F_{dl}$ and $T_{10} = eT_9 = e^4F_{dl}$.

The immediate first result is that $F_{dw} = \frac{F_{dl}}{e^4}$ when lifting and $F_{dw} = e^4F_{dl}$ when lowering. We can therefore infer that: $\forall v_{tb} > 0, F_{dw} = \frac{F_{dl}}{e^n}$ and $\forall v_{tb} < 0, F_{dw} = e^nF_{dl}$ when n is the number of lines supporting the traveling blocks.

If we write the force equilibrium on the traveling equipment, we have:

$$T_3 + T_4 + T_7 + T_8 = F_{tb}$$

When lifting the traveling equipment:

$$F_{tb} = F_{dl} + \frac{F_{dl}}{e} + \frac{F_{dl}}{e^2} + \frac{F_{dl}}{e^3} = F_{dl}\left(1 + \frac{1}{e} + \frac{1}{e^2} + \frac{1}{e^3}\right) = F_{dl}\frac{1 - \frac{1}{e^4}}{1 - \frac{1}{e}} = F_{dl}e\frac{1 - \frac{1}{e^4}}{e - 1}$$

Generalizing to n lines supporting the traveling equipment, we have:

$$\forall v_{tb} > 0, F_{tb} = F_{dl}e\frac{1 - \frac{1}{e^4}}{e - 1}$$

When lowering the traveling equipment:

$$F_{tb} = F_{dl} + eF_{dl} + e^2F_{dl} + e^3F_{dl} = F_{dl}(1 + e + e^2 + e^3) = F_{dl}\frac{1 - e^4}{1 - e}$$

The generalization to n lines supporting the traveling equipment gives:

$$\forall v_{tb} < 0, F_{tb} = F_{dl}\frac{1 - e^n}{1 - e}$$

Similarly, the force equilibrium on the crown blocks is:

$$T_1 + T_2 + T_5 + T_6 + T_9 + T_{10} = F_d$$

which can be expanded when lifting up the traveling equipment as:

$$F_d = F_{dl} + F_{dl} + \frac{F_{dl}}{e} + \frac{F_{dl}}{e^2} + \frac{F_{dl}}{e^3} + \frac{F_{dl}}{e^4} = F_{dl}\left(1 + 1 + \frac{1}{e} + \frac{1}{e^2} + \frac{1}{e^3} + \frac{1}{e^4}\right) = F_{dl}\left(1 + \frac{1 - \frac{1}{e^5}}{1 - \frac{1}{e}}\right)$$

$$= F_{dl}\left(1 + e\frac{1 - \frac{1}{e^5}}{e - 1}\right) = F_{dl}\left(\frac{e - 1 + e - \frac{1}{e^4}}{e - 1}\right) = F_{dl}\left(\frac{1 + \frac{1}{e^4} - 2e}{1 - e}\right)$$

By generalization to n lines supporting the traveling equipment, we obtain:

$$\forall v_{tb} > 0, F_d = F_{dl}\left(\frac{1 + \frac{1}{e^n} - 2e}{1 - e}\right)$$

For the lowering case, we expand the tensions in:

$$F_d = F_{dl} + F_{dl} + eF_{dl} + e^2F_{dl} + e^3F_{dl} + e^4F_{dl} = F_{dl}(1 + 1 + e + e^2 + e^3 + e^4)$$
$$= F_{dl}\left(1 + \frac{1 - e^5}{1 - e}\right) = F_{dl}\left(\frac{1 - e + 1 - e^5}{1 - e}\right) = F_{dl}\left(\frac{2 - e - e^5}{1 - e}\right)$$

The generalization to n lines supporting the traveling equipment gives:

$$F_d = F_{dl}\left(\frac{2 - e - e^{n+1}}{1 - e}\right)$$